Expanding the Scope of Ligand Substitution from [M($S_2C_2Ph_2$] (M = Ni^{2+}, Pd^{2+}, Pt^{2+}) to Afford New Classes of Heteroleptic Dithiolene Complexes

Antony Obanda,[†] Kristina Martinez,[†] Russell H. Schmehl,[†] Joel T. Mague,[†] Igor V. Rubtsov,[†] Samantha N. MacMillan,[‡] Kyle M. Lancaster,[‡] Stephen Sproules,[§] and James P. Donahue[†,*]

[†]Department of Chemistry, Tulane University, 6400 Freret St., New Orleans, Louisiana 70118.
[‡]Department of Chemistry and Chemical Biology, Cornell University, 162 Sciences Dr., Ithaca, New York 14853.
[§]University of Glasgow, School of Chemistry, University Avenue, Glasgow, Lanarkshire G12 8QQ, United Kingdom.

Abstract. The scope of direct substitution of dithiolene ligand from $[M(S_2C_2Ph_2)_2]$ (M = Ni^{2+} (**1**), Pd^{2+} (**2**), Pt^{2+} (**3**)) to produce heteroleptic species $[M(S_2C_2Ph_2)_2L_n]$ (n = 1, 2) has been broadened to include isonitriles and dithiooxamides in addition to phosphines and diimines. Collective observations regarding ligands that cleanly produce $[M(S_2C_2Ph_2)L_n]$, do not react at all, or lead to ill-defined decomposition identify soft σ donors as the ligand type capable of dithiolene substitution. Substitution of MeNC from $[Ni(S_2C_2Ph_2)(CNMe)_2]$ by L provides access to a variety of heteroleptic dithiolene complexes not accessible from **1**. Substitution of dithiolene ligand from **1** involves net redox disproportionation of the ligands from radical monoanions, $^{-}S,^{\cdot}SC_2Ph_2$, to ene-dithiolate and dithione, the latter of which is an enhanced leaving group that is subject to further irreversible reactions.

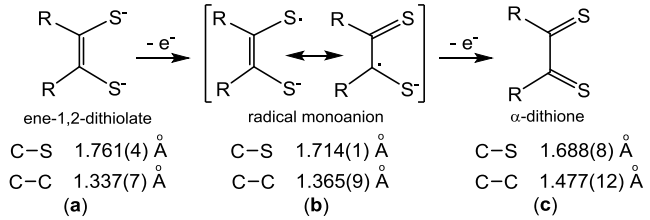

Scheme 1. Redox levels for a dithiolene ligand with typical C−S and C−C bond lengths indicated. Bond lengths for (**a**) and (**b**) are those found in $[Ni(S_2C_2Me_2)_2]^n$ for n = 2-, 0, respectively.[3] Bond lengths for (**c**) are those reported for $[Ni(Me_2pipdt)_2]^{2+}$ (Me_2pipdt = 1,4-dimethylpiperazine-2,3-dithione).[4]

Introduction

The emergence of metallodithiolene chemistry as a distinctive subfield of inorganic coordination chemistry was driven by research aimed at understanding the electronic structures of homoleptic bis- and tris(dithiolene) complexes, which did not yield to classical formalisms for describing a d electron count. The seminal studies in this area by Gray, Holm, Schrauzer, and later by Wieghardt, provided the foundation upon which the general concepts of ligand redox non-innocence are now expressed.[1,2] **Scheme 1** illustrates the several redox states accessible to a dithiolene ligand even when coordinated to a transition metal ion.

At the time these early studies were being conducted, heteroleptic dithiolene complexes were also being reported, the first being mono(dithiolene) bis(phosphine) complexes of the Group 10 metals. Several approaches to this compound type were disclosed: Oxidative addition of dithiacyclobutene to $[Ni(CO)_2(PR_3)_2]$ (**Eq 1**);[5] substitution of halide by an ene-1,2-dithiolate salt (**Eq 2**);[5] displacement of dithiolene ligand from a bis(dithiolene) complex by phosphine (**Eq 3**).[6] The last of these approaches is the least obvious, inasmuch as the kinetic advantage of a chelating ligand is overtaken by monodentate ligands, even when the latter is present in sub-stoichiometric amounts. Although it has been applied in the synthesis of $[M(S_2C_2R_2)(diimine)]$ (M = Ni or Pt, R = CF_3 or Ph, diimine = phen, diazadiene, or bipy) complexes,[7-9] the reaction type of **Eq 3** has not been broadly investigated for its generality or for a better understanding of the factors that enable its occurrence. In this report, we present leading results from a systematic examination of this dithiolene displacement reaction, describe the properties of new sets of

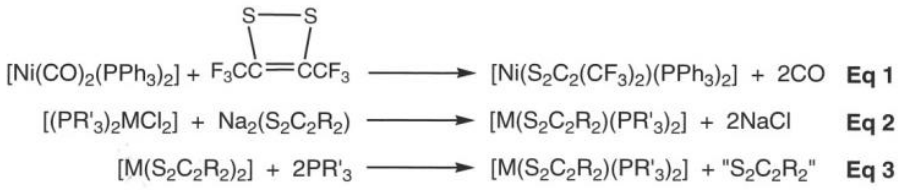

heteroleptic Group 10 dithiolene complexes, and provide insight into the ligand attributes necessary for this reactivity to occur and into the fate of the displaced dithiolene ligand.

Experimental

Physical Methods. UV-vis spectra were obtained at ambient temperature with a Hewlett-Packard 8452A diode array spectrometer, while IR spectra were taken either as pressed KBr pellets or as CH_2Cl_2 solutions with a Thermo Nicolet Nexus 670 FTIR instrument in absorption mode. All ^1H NMR spectra were recorded at 25 °C either with a Varian Unity Inova spectrometer (400 MHz) or with a Bruker Avance spectrometer (300 mHz). Spectra were referenced to the protonated solvent residual. Mass spectra (MALDI-TOF) were obtained with a Bruker Autoflex III instrument operating in positive ion mode. Electrochemical measurements were made with a CHI620C electroanalyzer workstation using a Ag/AgCl reference electrode, a platinum disk working electrode, Pt wire as auxiliary electrode, and [^{n}Bu$_4$N][PF_6] as the supporting electrolyte. Under these conditions, the Cp_2Fe^+/Cp_2Fe reduction consistently occurred at +540 mV, and all potentials are reported relative to this couple. Elemental analyses were performed by Midwest Microlab, LLC of Indianapolis, IN or by Galbraith Laboratories, Inc. of Knoxville, TN.

Emission spectra samples were prepared in a 4:5 propionitrile/butyronitrile solvent mixture and cooled to 77 K using liquid nitrogen. Time-resolved emission spectra (450 nm - 750 nm, 10 nm steps) were collected using an Applied Photophysics LKS 60 optical system. A 355 nm excitation (< 4 ns pulse) was provided by a Quantel Brilliant B Q-switched Nd:YAG laser equipped with frequency doubling and tripling crystals. A 0.2 neutral density filter (Thorlabs) was placed before the sample to decrease the power of the excitation light source to 10 mJ/ pulse. Detection at a right angle was accomplished using a single grating monochromator (Applied Photophysics 0.25m) with PMT detector (Hamamatsu R298). Emission decays were collected using linear oversampling with a 600 MHz Agilent Infiniium oscilloscope.

X-ray Absorption Spectroscopy (XAS). X-ray absorption spectra (XAS) were measured at the Stanford Synchrotron Radiation Lightsource (SSRL). Sulfur K-edge data were obtained using the 20-pole wiggler beamline 4-3. Detailed S K-edge data collection and normalization procedures were followed as previously described.[10] Data were averaged using *EXAFSPAK*[11] and normalized by subtracting the spline and normalizing the postedge to 1.0. The S K pre-edge

features were modeled with lineshapes having fixed mixing ratios (1:1) of Lorentzian and Gaussian functions (pseudo-Voigt) using the program *EDG_FIT*.[11]

Syntheses. The $[M(S_2C_2Ph_2)_2]$ ($M = Ni^{2+}$, Pd^{2+}, Pt^{2+}) starting materials were synthesized according to the procedure outlined by Schrauzer and Mayweg.[6] Methyl isonitrile was prepared by the dehydration of *N*-methylformamide,[12] and its density was experimentally determined to be 0.78 g/mL. The *tert*-butyl and phenyl isonitriles were synthesized via the phase-transfer Hofmann-carbylamine reaction.[13] The 1,4-diisopropylpiperidine-2,3-dithione ($^{i}Pr_2$pipdt) ligand was synthesized by a modification of the procedure documented by R. Isaksson *et al.*[14] The IPr-HBF_4 (IPr = 1,3-bis(2,6-diisopropylphenyl)imidazol-2-ylidene) protected form of the carbene ligand was prepared and unmasked under N_2 following the protocol documented by Bantreil and Nolan.[15] The free IPr ligand was stored in the glovebox. Purifications by column chromatography were conducted in open air using 60−230 μm silica (Dynamic Adsorbents) and solvents used as received from Fisher Scientific. The numbering system employed hereafter in compound identification is that defined in **Scheme 1**. The following descriptions of synthesis procedures are representative; forthcoming reports will fully detail the preparations and physical characterizations of all new compounds.

$[Ni(S_2C_2Ph_2)(CNMe)_2]$, **4a**. Methyl isonitrile (0.020 mL, 0.0156 g, 0.38 mmol) was added to a solution of **1** (0.100 g, 0.184 mmol) in CH_2Cl_2 (25 mL). The mixture was stirred at 25 °C for 5 h, after which time the solvent was removed under reduced pressure. The dark blue residual solid was applied directly to the top of a silica gel column packed as a slurry in hexanes. Flash elution with 1:1 CH_2Cl_2:hexanes moved a dark green band of unreacted **1**, followed by a blue band of **4a**. Following collection of the fraction containing **1**, continued elution with 2:1 CH_2Cl_2:hexanes enabled collection of the blue fraction of **4a**. This blue fraction was taken to dryness under reduced pressure. The residual solid was washed with *n*-pentane and then redissolved in a minimal volume of CH_2Cl_2. The resulting solution was filtered through a Celite pad and reduced to dryness again. Following drying of the solid for 1 h under reduced pressure, crystallization was accomplished by slow diffusion of Et_2O vapor into a concentrated dichloromethane solution. Yield: 0.051 g, 79%. R_f = 0.11 (2:1 CH_2Cl_2 :hexanes). ^{1}H NMR (δ, ppm in CD_2Cl_2): 7.16-7.09 (m, 6H, Ph), 7.08-7.05 (m, 4H, Ph), 3.36 (s, 6H, Me). Solution IR (CH_2Cl_2, cm^{-1}): 2228 (vs, CN_{sym}), 2214 (vs, CN_{asym}). Absorption spectrum (CH_2Cl_2) λ_{max} nm (ε_M): 274 (31700), 348

(17200), 445 (240), 604 (300). Cyclic voltammetry: **4a** − e^- → [**4a**]$^{1+}$, -0.02 V. Anal. Calcd for $C_{18}H_{16}N_2S_2Ni$: C, 56.42; H, 4.22; N, 7.31. Found: C, 56.20; H, 3.92; N, 7.24.

[Pd($S_2C_2Ph_2$)(CN^tBu)$_2$], **5c**. Procedures similar to that described above for the synthesis and purification of **4a** were employed but with 0.040 mL (0.338 mmol) of *tert*-butylisonitrile and 0.100 g (0.169 mmol) of **2** in 25 mL CH_2Cl_2, ultimately affording red crystals of **5c**. Yield: 0.056 mg, 71%. R_f = 0.38 (2:1 CH_2Cl_2:hexanes). ^{1}H NMR (δ, ppm in CD_2Cl_2): 7.14-7.11 (m, 6H, Ph), 7.09-7.06 (m, 4H, Ph), 1.56 (s, 18H, ^{t}Bu). Solution IR (CH_2Cl_2, cm^{-1}): 2213 (vs, CN_{sym}), 2197 (vs, CN_{asym}). Absorption spectrum (CH_2Cl_2) λ_{max} nm (ε_M): 240 (32500), 336 (17300), 498 (620), 419 (860). Cyclic voltammetry: **5c** − e^- → [**5c**]$^{1+}$, +0.06 V.

[Pt($S_2C_2Ph_2$)($CNPh$)$_2$], **6e**. Procedures similar to that described above for the synthesis and purification of **4a** were employed but with 0.28 mL (2.95 mmol) of phenylisonitrile and 0.100 g (0.147 mmol) of **3** in CH_2Cl_2 (25 mL), ultimately producing yellow crystals of **6e**. Yield: 0.03770 g, 59%. R_f = 0.66 (2:1 CH_2Cl_2:hexanes). ^{1}H NMR (δ, ppm in CD_2Cl_2): 7.53-7.48 (m, 10H, PhCN), 7.16-7.14 (m, 6H, Ph), 7.13-7.11 (m, 4H, Ph). Solution IR (CH_2Cl_2, cm^{-1}): 2199 (vs, CN_{sym}), 2172 (vs, CN_{asym}). Absorption spectrum (CH_2Cl_2) λ_{max} nm (ε_M): 274 (35800), 390 (4070). Cyclic voltammetry: **6e** − e^- → [**6e**]$^{1+}$, +0.19 V. Anal. Calcd for $C_{28}H_{20}N_2S_2Pt$: C, 52.24; H, 3.14; N, 4.35. Found: C, 52.52; H, 3.15; N, 4.50.

[Ni($S_2C_2Ph_2$)(^{i}Pr$_2$pipdt)], **7**. A solution of ^{i}Pr$_2$pipdt (0.300 g, 1.30 mmol) in MeC≡N (5 mL) was added to a solution of **1** (0.708 g, 1.30 mmol) in CH_2Cl_2 (25 mL), and the resulting mixture was stirred for 6 h at 25 °C. Unreacted starting material and excess ligand were separated from the product by flash column chromatography on silica (2:1 CH_2Cl_2:hexanes). Dark green **7** was eluted subsequently using 100% CH_2Cl_2. The solvent was removed under reduced pressure, and the residual solid was washed with *n*-pentane. Following redissolution in a minimal volume of CH_2Cl_2 and filtration of that solution through Celite, **7** was crystallized by the slow introduction of Et_2O by vapor diffusion. Yield: 0.281 g, 63%. R_f = 0.24 (CH_2Cl_2). ^{1}H NMR (δ, ppm in CD_2Cl_2): 7.26-7.24 (m, 6H, Ph), 7.14-7.12 (m, 4H, Ph), 3.33-3.31 (m, 2H, ^{i}Pr), 3.37-3.35 (t, 4H, CH_2), 1.40-1.39 (d, 12H, ^{i}Pr). Absorption spectrum (CH_2Cl_2) λ_{max} nm (ε_M): 319 (11900), 940 (6020). Cyclic voltammetry: **7** − e^- → [**7**]$^{1+}$, -0.19 V; **7** + e^- → [**7**]$^{1-}$, -1.30 V. MALDI MS: *m/z* $C_{24}H_{28}N_2NiS_4$: 530.049, Observed: 530.024. Anal. Calcd for $C_{24}H_{28}N_2NiS_4$: C, 54.23; H, 5.32; N, 5.27. Found: C, 54.06; H, 5.28; N, 5.27.

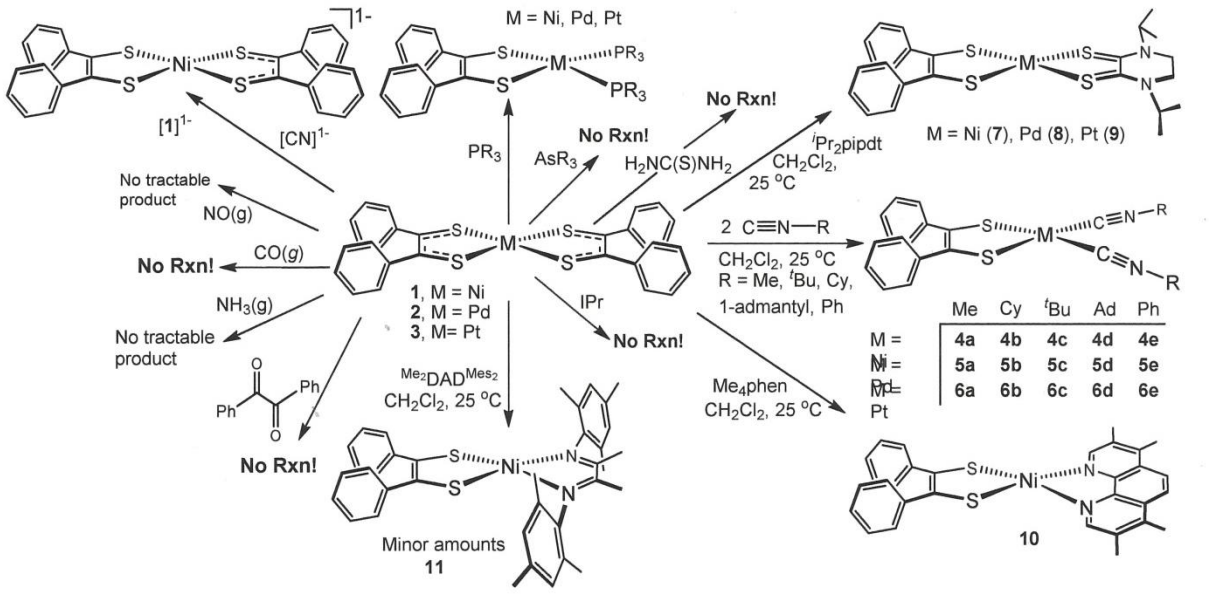

Scheme 2. Dithiolene ligand substitution reactions from $[M(S_2C_2Ph_2)_2]$ (M = Ni^{2+}, Pd^{2+}, Pt^{2+}).

[Ni(S$_2$C$_2$Ph$_2$)(Me$_4$phen)], **10**. A solution of 3,4,7,8-tetramethyl-1,10-phenanthroline (0.050 g (0.189 mmol) was introduced to a solution of **1** (0.189 mmol) in CH_2Cl_2 (25 mL), and the resulting mixture was stirred overnight at 25°C. The unreacted starting material and excess ligand were separated from the product by flash column chromatography (2:1 CH_2Cl_2 : hexanes) followed by elution of the dark purple product using 100% CH_2Cl_2. The solvent was removed under reduced pressure, and the crude solid product was washed with *n*-pentane. The product was dissolved in a minimum amount of 1,2-dichloroethane, filtered through Celite and crystallized by slow diffusion of *tert*-butyl methyl ether vapor into the concentrated solution of 1,2-dichloroethane. Yield: 0.04436 g, 71%. R_f = 0.67 (CH_2Cl_2). ^{1}H NMR (δ, ppm in CD_2Cl_2): 8.74 (s, 2H, phen), 7.98 (s, 2H, phen), 7.19-7.16 (m, 6H, Ph), 7.10-7.08 (m, 4H, Ph), 2.62 (s, 6H, Me), 2.49 (s, 6H, Me). Absorption spectrum (CH_2Cl_2) λ_{max} nm (ε_M): 275 (32000), 367 (6500), 567 (5200), 868 (2850). MALDI MS: *m/z* $C_{30}H_{26}N_2NiS_2$: 538.084, Observed: 538.393.

[Ni(S$_2$C$_2$Ph$_2$)(^{Me_2}**DAD**^{Mes_2}**)]**, **11**. A solid portion of *N*,*N'*-dimesityl-2,3-butanediimine (diazadiene, $^{Me_2}DAD^{Mes_2}$) (0.023 g, 0.070 mmol) was added to a CH_2Cl_2 solution of **4a** (0.0270 g, 0.070 mmol), which occasioned an immediate color change from blue to green. The resulting mixture was allowed to stir for 3 h at 25°C, after which time the solvent was removed under reduced pressure. The residual solid was purified by chromatography on a silica column packed as a slurry in hexanes. Unreacted diazadiene ligand was separated first by flash elution with 100% hexanes; continued elution with the 2:1 CH_2Cl_2:hexanes moved **11** as a green band.

Following collection of **11**, the solvent was removed under reduced pressure, and the remaining solids were washed with *n*-pentane. Redissolution in a minimal amount of CH_2Cl_2, filtration through Celite and slow crystallization by introduction of Et_2O via vapor diffusion afforded **11** as green-yellow columns. Yield: 0.0444 g, 67%. R_f = 0.80 (2:1 CH_2Cl_2:hexanes). ^{1}H NMR (δ, ppm in CD_2Cl_2): 7.03-7.02 (m, 6H, Ph), 7.01-6.99 (m, 4H, Ph), 6.92 (s, mesityl CH), 2.35 (s, 6H, mesityl CH_3), 2.33 (s, 12H, mesityl CH_3), 2.27 (s, 6H, diene CH_3). Absorption spectrum (CH_2Cl_2) λ_{max} nm (ε_M): 234 (44000), 270 (17500), 316 (13900), 478 (1200), 776 (6600). Cyclic voltammetry: **11** − e^- → [**11**]$^{1+}$, 0.00 V; **11** + e^- → [**11**]$^{1-}$, -1.71 V. MALDI MS: *m/z* $C_{36}H_{38}N_2NiS_2$: 620.183, Observed: 620.058.

[Ni($S_2C_2Ph_2$)(IPr)(CNMe)], **12**. Under a protecting atmosphere of N_2, a 25 mL Schlenk flask was charged with a Teflon-coated stir bar, free IPr ligand (0.050 g, 0.130 mmol), and anhydrous THF (10 mL) delivered via gas-tight syringe. To this homogeneous stirring solution was then added via cannula a solution of **4a** (0.020 g, 0.052 mmol) in 10 mL THF. The resulting purple-colored mixture was stirred at 25°C overnight under N_2. The solvent was removed under reduced pressure, and the residual solid was purified by flash column chromatography from a silica column eluted with 2:1 CH_2Cl_2:hexanes. Crystallization of the purple solid obtained after removal of the eluting solvents was accomplished by the diffusion of hexanes vapor into a concentrated 1,2-dichloroethane solution. Yield: 0.0272 g, 71%. R_f = 0.18 (2:1 CH_2Cl_2: hexanes). ^{1}H NMR (δ, ppm in CD_2Cl_2): 7.58 (s, 2H, IPr C(*H*)=C(*H*), 7.57-7.54 (m, 6H, dithiolene Ph), 7.41-7.19 (m, 4H, dithiolene Ph), 7.15-7.00 (m, 6H, IPr Ph), 3.17 (s, 3H, isonitrile C*H*$_3$), 2.89-2.97 (m, 4H, ^{i}Pr C*H*), 1.34 (d, 12H, ^{i}Pr C*H*$_3$), 1.13 (d, 12H, ^{i}Pr C*H*$_3$). Solution IR (CH_2Cl_2, cm^{-1}): 2190 (vs, CN). Absorption spectrum (CH_2Cl_2) λ_{max} nm (ε_M): 350 (11600), 560 (410), 867 (120). Cyclic voltammetry: **12** − e^- → [**12**]$^{1+}$, -0.13 V; [**12**]$^{1+}$ − e^- → [**12**]$^{2+}$, ~+0.76 V, irreversible. MALDI MS: *m/z* $C_{43}H_{50}N_3NiS_2$: 729.272, Observed: 729.182. Anal. Calcd for $C_{43}H_{49}N_3NiS_2$: C, 70.68; H, 6.76; N, 5.75. Found: C, 70.60; H, 7.31; N, 5.46.

[Et_4N]$_2$[Ni($S_2C_2Ph_2$)($CN)_2$], [Et_4N]$_2$[13]. Under an atmosphere of Ar, tetraethylammonium cyanide (0.650, 4.2 mmol) was added to a solution of **4a** (0.800 g, 2.1 mmol) in CH_3NO_2 (15 mL). This mixture was heated to 100 °C with stirring, and a color change from blue to orange was observed after several minutes. After 30 min of heating and stirring, the reaction mixture was cooled to ambient temperature. To assist completion of the ligand substitution, the displaced MeNC was collected in a liquid N_2-cooled trap under lowered pressure until the volume of the

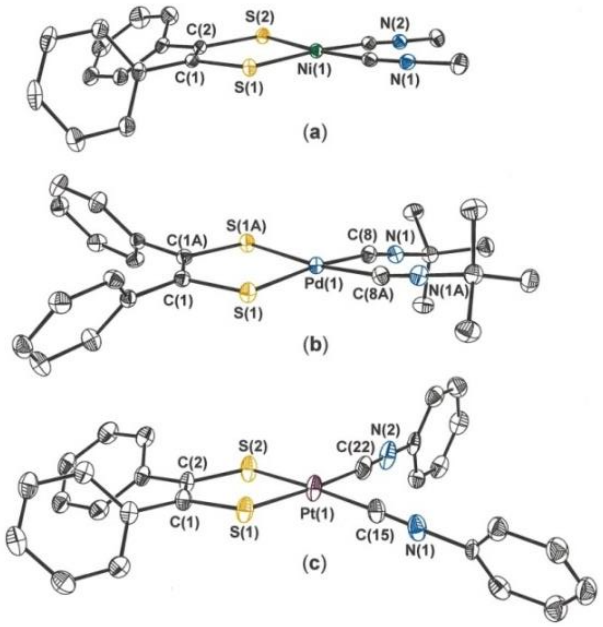

Figure 1. Thermal ellipsoid plots (50%) of (**a**) **4a**, (**b**) **5c**, (**c**) **6e**. Hydrogen atoms are omitted for clarity.

solution was reduced by ~1 mL. Heating at 100 °C and stirring under Ar were then continued overnight. Following complete cooling to ambient temperature, the CH_3NO_2 was fully removed under vacuum to afford a red-brown solid residue. This residue was washed with Et_2O (2 x 10 mL) and then redissolved in 10 mL MeCN. The MeCN solution was filtered through a celite pad into a Schlenk tube, and the filtrate was then frozen. An equal volume of Et_2O was added via syringe, and the tube was allowed to thaw slowly and the solvents to mix by diffusion over a period of days. Red-brown crystals of $[Et_4N]_2$[**13**] appeared at the solvent interface after several days and were isolated by decanting the mother liquor. The crystals remaining were washed with *n*-pentane and dried under vacuum. Yield: 0.12 g, 0.196 mmol, 9.3%. ^{1}H NMR (δ, ppm in CD_2Cl_2): 7.25-7.04 (m, 6H, Ph), 7.03-7.25 (m, 6H, Ph), 3.46-3.38 (q, 16H, $N(CH_2CH_3)_4^+$), 1.39-1.33 (t, 24H, $N(CH_2CH_3)_4^+$). Solution IR (CH_3CN, cm^{-1}): 2100 (vs, $C{\equiv}N_{sym}$), 2095 (vs, $C{\equiv}N_{asym}$). Absorption spectrum (CH_2Cl_2) λ_{max} nm (ε_M): 490 (220), 380 (5380).

4,5-diphenyl-1,3-dithiol-2-cyclohexylimine. Four equivalents of cyclohexylisonitrile (0.05 mL, 0.368 mmol) were added to a dilute solution of **1** (0.0500 g, 0.092 mmol) in CH_2Cl_2 (500 mL). The mixture was stirred for 5 h at 25°C, after which time the formation of the product was confirmed by TLC (*vide infra*) with UV lamp visualization. The solvent was then reduced in volume using a rotary evaporator, and a minimal amount of silica (~0.5 g) was added to the

Table 1. Crystal and refinement data for compounds [Et_4N][**1**], **4a**, **5c**, **6e**, **7**, **11**, **12**·$ClCH_2CH_2Cl$, $[Et_4N]_2$[**13**], and 4,5-diphenyl-1,3-dithiol-2-cyclohexylimine, **14**.

compound	[Et_4N][**1**]	**4a**	**5c**	**6e**	**7**
solvent	none	none	none	none	none
formula	$C_{36}H_{40}NNiS_4$	$C_{18}H_{16}N_2NiS_2$	$C_{24}H_{28}N_2PdS_2$	$C_{28}H_{20}N_2PtS_2$	$C_{24}H_{28}N_2NiS_4$
fw	673.64	383.16	515.00	643.67	531.43
xtl system	orthorhombic	orthorhombic	monoclinic	triclinic	triclinic
space grp	$Pca2_1$	$Pbca$	$C2/c$	$P\bar{1}$	$P\bar{1}$
color,	red	red	orange	pale yellow	yellow-green
habit	plate	block	block	plate	plate
a, Å	16.1524(8)	7.9345(7)	20.689(2)	9.9489(16)	9.4720(7)
b, Å	7.1528(4)	26.862(2)	16.1770(16)	10.0740(7)	9.6769(8)
c, Å	28.4304(14)	32.836(3)	7.4404(7)	12.291(2)	15.3820(12)
α, deg.	90	90	90	89.296(2)	80.506(4)
β, deg.	90	90	101.275(1)	88.688(2)	81.113(3)
γ, deg.	90	90	90	82.354(2)	61.819(3)
V, Å^3	3450.0(3)	6998.6(10)	2442.1(4)	1220.6(3)	1220.99(17)
T, K	150	100	100	150	100
Z	4	16	4	2	2
R1[a]	0.0376	0.0341	0.0194	0.0340	0.0308
wR2[b]	0.0854	0.0813	0.0515	0.0696	0.0768
GoF	0.992	1.037	1.109	0.947	1.020

compound	**11**	**12**	$[Et_4N]_2$[**13**]	**14**
solvent	none	$ClCH_2H_2Cl$	none	none
formula	$C_{36}H_{38}N_2NiS_2$	$C_{45}H_{53}Cl_2N_3NiS_2$	$C_{32}H_{50}N_4NiS_2$	$C_{21}H_{21}NS_2$
fw	621.51	829.63	613.59	351.51
xtl system	orthorhombic	orthorhombic	monoclinic	monoclinic
space grp	$P2_12_12_1$	$Pna2_1$	$P2_1/c$	$P2_1/c$
color,	green-yellow	red	orange	colorless
habit	column	block	plate	column
a, Å	12.1471(10)	16.2425(9)	21.587(3)	9.5063(6)
b, Å	15.0979(11)	21.3543(12)	7.8930(9)	19.2814(12)
c, Å	17.4013(13)	12.5518(7)	19.660(9)	9.8563(6)
α, deg.	90	90	90	90
β, deg.	90	90	105.254(2)	102.926(1)
γ, deg.	90	90	90	90
V, Å^3	3191.3(4)	4353.6(4)	3231.8(7)	1760.83(19)
T, K	100	100	100	100
Z	4	4	4	4
R1[a]	0.0330	0.0462	0.0389	0.0383
wR2[b]	0.0768	0.1192	0.1004	0.1026
GoF	0.996	1.074	1.067	1.110

[a]$R1 = \Sigma||F_o| - |F_c||/\Sigma|F_o|$, $I > 2\sigma(I)$. [b]$R_w = \{[\Sigma w(F_o^2 - F_c^2)/\Sigma w(F_o^2)^2\}^{1/2}$; $w = 1/[\sigma^2(F_o^2) + (xP)^2]$, where $P = (F_o^2 + 2F_c^2)/3$, $I > 2\sigma(I)$..

flask. The resulting slurry was taken to dryness. The dry-loaded silica was applied directly to the top of a silica gel column packed as a slurry in hexanes, and the column was then eluted with 1:1 CH_2Cl_2:hexanes. A fraction of unreacted **1** was collected. The column was continued with the same solvent mixture until incipient elution of **4b** (~35 mL). This portion of the eluent was then taken to dryness under reduced pressure, and the residual solid was washed with *n*-pentane. Crystallization was accomplished by diffusion of Et_2O vapor into a CH_2Cl_2 solution, yielding

Table 2. Selected bond lengths (Å), angles (deg.) for **1a**, **2c**, **3e**, and $[\mathbf{13}]^{2-}$.[a]

	1a	**2c**	**3e**	$[\mathbf{13}]^{2-}$
M−C_{ave}	1.8551[9]	1.9955(13)	1.965[3]	1.8705[12]
M−S_{ave}	2.1427[3]	2.2604(3)	2.2748[7]	2.1573[4]
Δ^b	0.288	0.265	0.310	0.287
S−C_{ave}	1.7649[8]	1.7606(12)	1.764[3]	1.7667[11]
C−$C_{chelate}$	1.348[1]	1.351(2)	1.345(5)	1.345(2)
C−M−C	89.91[5]	93.33(7)	92.13(16)	90.70(7)
S−M−S	90.478[13]	88.028(16)	88.53(3)	91.512(17)
S−M−$C_{cis,ave}$	90.18[3]	89.92(4)	89.72[8]	89.99[4]
S−M−$C_{trans,ave}$	173.44[3]	171.28(4)	175.40[9]	176.67[4]
θ^c	6.9, 12.2	11.7	4.0	4.7

[a]Chemically identical, crystallographically independent values are averaged. Square brackets represent uncertainties propagated according to the general formula for uncertainty in a function of several variables, as detailed in Taylor, J. R. *An Introduction to Error Analysis*; University Science Books: Sausalito, California, 1997, pp 73-77. [b]$\Delta = (M{-}S_{ave}) - (M{-}C_{ave})$. [c]θ = angle between MS_2 and MC_2 planes.

clear to off-white crystals. Yield: 0.0032 g, 9.89%. Melting point = 143-147 °C. R_f = 0.24 (1:1 CH_2Cl_2:hexanes). ^{1}H NMR (δ, ppm in CD_2Cl_2): 7.21-7.10 (m, 6H, Ph), 7.10-7.09 (m, 4H, Ph), 3.64–3.62 (m, 1H, Cy), 1.96-1.49 (m, 10H, Cy). Solution IR (CH_2Cl_2, cm^{-1}): 1600 (vs, C=N).

Results and Discussion

A motivating premise to this study was that ligands possessing the good σ-donor and modest π-acid characteristics of a typical phosphine would be those most likely to substitute dithiolene in the fashion illustrated in **Eq 3**. Arsines notably fail to react with **1** under the mild conditions in which phosphines, with the same set of ancillary alkyl or aryl groups, readily displace a dithiolene ligand (**Scheme 2**). Isonitriles, however, are plausible candidates that meet the criterion of holding phosphine-like basicity and π-acidity. Solutions of $[M(S_2C_2Ph_2)_2]$ ($M = Ni^{2+}$, Pd^{2+}, Pt^{2+}) in CH_2Cl_2 readily react with C≡N−R (R = Me, Cy, ^{t}Bu, 1-adamantyl, Ph) to afford $[M(S_2C_2Ph_2)(C{\equiv}N{-}R)_2]$ ($M = Ni^{2+}$, **4a-e**; $M = Pd^{2+}$, **5a-e**; $M = Pt^{2+}$, **6a-e**) in yields of ~70%. The only previously reported Group 10 compounds of this type are $[M(S_2C_2(CN)_2)(C{\equiv}NMe)_2]$, which have been prepared by addition of MeNC, followed by $Na_2[S_2C_2(CN)_2]$, to aqueous $NiCl_2$[16] or MCl_4^{2-} ($M = Pd^{2+}$, Pt^{2+})[17] solutions. Structural characterizations of $[M(S_2C_2(CN)_2)(C{\equiv}NMe)_2]$ ($M = Ni^{2+}$, Pd^{2+}) by X-ray crystallography have been reported,[16] while a structure of $[Pt(S_2C_2(CN)_2)(C{\equiv}NMe)_2]$ was later described as a 1:1 co-crystallite with $(NC)_2C_2S_2C{=}NMe$ in a sample prepared serendipitously by the reaction of $[Pt(C{\equiv}NMe)_4][PF_6]_2$ with $[^n Bu_4N]_2[Cu(S_2C_2(CN)_2)_2]$.[18] Heteroleptic dithiolene-isonitrile compounds that have been reported with other transition metals include $[Mo(S_2C_2H_2)_2(C{\equiv}N{}^tBu)_2]$,[19]

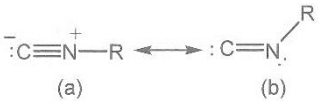

Scheme 3. Resonance forms of the isonitrile ligand.

$[W(S_2C_2Me_2)_2(C{\equiv}N^tBu)_2]$,[20] $[M(\text{arene-1,2-dithiolate})(C{\equiv}NR)_2]$ (M = Mo,[19,21] W[22]) and $[Ru(S_2C_6H_4)(C_6Me_6)(C{\equiv}N^tBu)]$,[23] but none of their syntheses proceeds by displacement of dithiolene ligand from a homoleptic compound by C≡NR.

Compounds **4a**-**e**, **5a**-**e**, and **6a**-**e** are air-stable and amenable to purification by column chromatography on silica and to crystallization by vapor diffusion techniques. Representative examples (**4a**, **5c**, **6e**) have been characterized structurally by X-ray crystallography; thermal ellipsoid plots and crystal data are presented in **Figure 1** and **Table 1**, respectively. The structural data, summarized as averaged values where possible, reveal the dithiolene ligands to be fully reduced and show the expected tendency toward greater square planarity, gauged by the angle (θ) between C_2M and S_2M planes, as one moves from Ni to Pd to Pt (**Table 2**).

The C≡N−R functional group is a useful reporter in the vibrational spectra of these compounds. **Table 3** presents the symmetric and anti-symmetric stretching frequencies for these compounds in CH_2Cl_2 solution alongside values for the free isonitrile ligand. For fixed M, $\upsilon_{C\equiv N}$ in the coordination compounds trend in the same way as, but occur at markedly higher energies than, the corresponding free ligands. This observation indicates an *absence* of metal-to-ligand π-backbonding and instead shows that the divalent metal ion accentuates, presumably by an inductive effect, limiting form (**a**) of the isonitrile ligand in **Scheme 3**, which maximizes the C-N bond order.[24]

Table 3. Symmetric and antisymmetric υ_{CN} (cm^{-1}) for $[M(S_2C_2Ph_2)(CNR)_2]$ compounds in CH_2Cl_2.

	Ni	Pd	Pt	Free ligand
MeNC	2214, 2228	2230, 2246	2223, 2246	2168
CyNC	2189, 2204	2203, 2217	2202, 2230	2144
^{t}BuNC	2180, 2197	2197, 2213	2188, 2214	2140
AdNC	2175, 2196	2198, 2211	2192, 2219	2133
PhNC	2162, 2182	2182, 2198	2172, 2199	2130

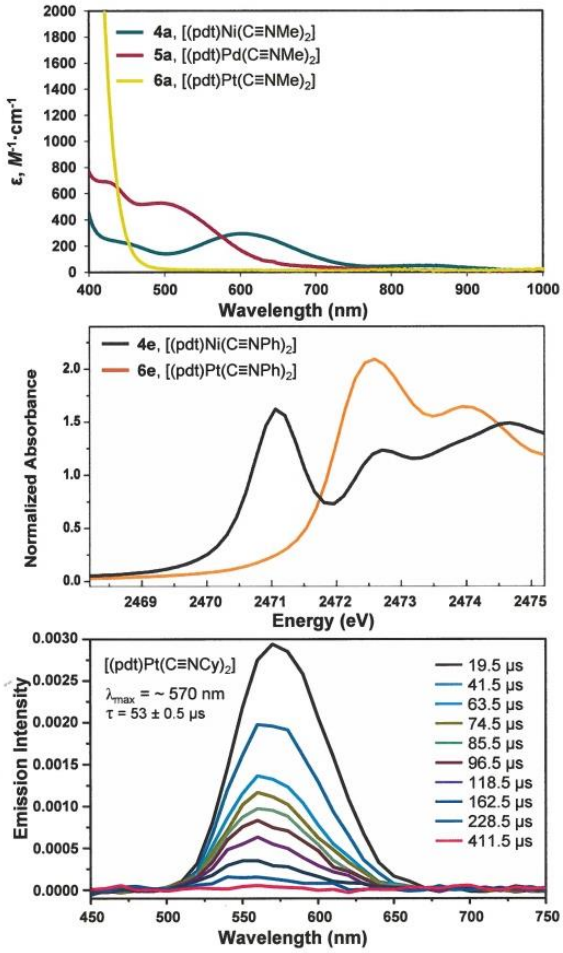

Figure 2. UV-vis spectra of **4a**, **5a**, **6a** in CH_2Cl_2 (top); S K-edge X-ray absorption spectra of **4e**, **6e** (middle); time-resolved emission spectrum of **6b** in MeCN (bottom). pdt = phenyl-substituted dithiolene ligand.

Compounds 4a-d manifest a characteristic blue color of modest intensity arising from a near invariant band at 600 nm (639 for 4e). This transition is a HOMO → LUMO excitation, the former MO being composed largely from a dithiolene C_2S_2 π-type MO and the latter being a σ* combination of the metal d_{x2-y2} and ligand orbitals. The shift to lower energy for **4e** is attributed to a delocalizing effect by the phenyl substituent upon the C≡N multiple bond. Compounds **5a-e** reveal spectral features uniformly shifted ~100 nm to higher energy, which imparts a distinctive red hue to their solutions. The effect arises from the inherently higher energy of the Pd 4d orbitals compared to their Ni 3d counterparts and continues with the Pt series (**6a-e**), which are yellow (**Figure 2**, top). The sulfur K-edge X-ray absorption spectra for **4a-e** and **6a-e** (**Figure 2**, middle) trend in a way that is qualitatively similar to the visible absorption spectra. The lowest

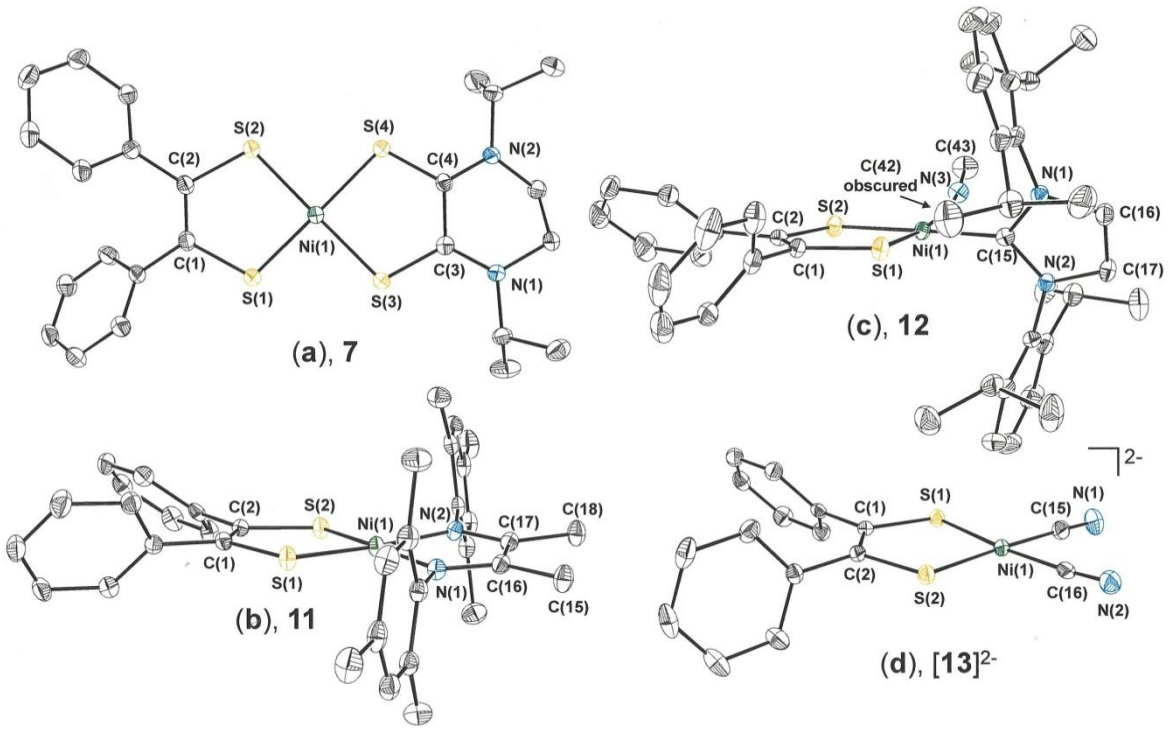

Figure 3. Thermal ellipsoid images of **7** (**a**), **11**, (**b**), **12** (**c**) and [**13**]$^{2-}$ (**d**) at the 50% level. Hydrogen atoms are omitted for clarity.

energy band is a superposition of S 1s → LUMO, LUMO+1 transitions. This band is well-separated from the rising edge energy for M= Ni, but for M = Pt, an analogous shift to higher energy by 1 – 1.5 eV produces significant overlap with excitations attributed to intraligand dithiolene transitions.[25]

Compounds **6a-e** exhibit yellow luminescence in low temperature glasses. Time-resolved emission spectra of the complexes in propionitrile/butyronitrile (4:3) at 77 K (λ_{ex} = 355 nm) have maxima between 550 and 600 nm and excited state lifetimes of 55 ± 3 μs for **6a** and **6c** (**Figure 2**, bottom). The arylisocyanide complex, **6e**, has an emission maximum approximately 20 nm to the red of the alkyl derivatives and a much shorter excited state lifetime (1.2 μs). The combination of spectroscopic and computational results suggests the emissive state is either of dithiolene (nb) to metal (σ*) or dithiolene to metal-isocyanide (σ*) charge transfer character. Given the long lifetimes, the emitting state is very likely of triplet spin multiplicity. Related dithiolene-diimine complexes are known to be similarly emissive,[26] but typically with lower energy emission maxima, and have been subject to considerable study as chromophores in light-to-electricity[7,27-29] or light-to-chemical energy conversion systems[30-32] and as sensors of various

Table 4. Oxidation potentials (V) for $[M(S_2C_2Ph_2)(C{\equiv}NR)_2] - e^- \rightarrow [M(S_2C_2Ph_2)(C{\equiv}NR)_2]^+$ in CH_2Cl_2 vs. Cp_2Fe^+/Cp_2Fe with 0.10 *M* $[Bu_4N][PF_6]$ supporting electrolyte.

	Ni	Pd	Pt
MeNC	-0.02	+0.07	+0.10
CyNC	+0.02	+0.07	+0.13
^{t}BuNC	+0.05	+0.06	+0.12
AdNC	+0.03	+0.05	+0.10
PhNC	+0.08	+0.13	+0.19

sorts.[33] Preliminarily, for reasons not yet unidentified, room temperature solutions of 6a-e are not emissive.

As is typically observed for $[M(S_2C_2R_2)(PR'_3)_2]$ complexes, compounds **4a-e**, **5a-e**, **6a-e** display as single reversible oxidation followed by an irreversible oxidation process at higher potentials (**Table 4**). The reversible oxidation is attributed to oxidation of the dithiolene ligand to a radical monoanion from an ene-1,2-dithiolate: $Ph_2C_2S_2^{2-} + e^- \rightarrow Ph_2C_2S^{\cdot},S^-$. In all cases, the PhNC complexes have the higher potentials for this process, possibly because the phenyl substituent exerts a modest delocalizing effect upon the charge density for the molecule as a whole. For a fixed ligand set, oxidation potentials increase in going from $Ni^{2+} \rightarrow Pd^{2+} \rightarrow Pt^{2+}$, suggesting greater positive character to the heavier metal ions and more covalency between metal and ligand in the nickel complexes.

Use of a dithiooxamide ligand, such as the readily prepared ^{i}Pr$_2$pipdt (^{i}Pr$_2$pipdt = 1,4-diisopropylpiperidine-2,3-dithione), also results in facile substitution to afford mixed ene-dithiolate, α-dithione complexes (**Scheme 2**, **7-9**), which feature distinctive, low energy inter-ligand intervalence charge transfer transitions. **Figure 3** presents the structure of the M = Ni compound (**7**), as determined by X-ray diffraction. Compounds of this type, so called "push-pull" complexes, have elicited interest for possible applications arising from their nonlinear optical properties. Previously reported examples of this compound type have the $S{=}CS_2C_2S_2^{2-}$ (dimercaptoisotrithione ligand(2-), dmit) and have made by an alternate, less direct route involving the transfer of dmit(2-) from $[^n Bu_4N]_2[M(dmit)_2]$ to $[M(R_2pipdt)Cl_2]$ and displacement of Cl^- upon mixing solution samples.[34-36]

Ligands that do not displace dithiolene from $[M(S_2C_2Ph_2)_2]$ include $[C{\equiv}N]^{1-}$, which instead reduces the compound by one electron (**Scheme 2**), presumably forming cyanogen as byproduct. The $[Ni(S_2C_2Ph_2)_2]^{1-}$ anion was identified structurally as its Et_4N^+ salt.[37] Introduction of either

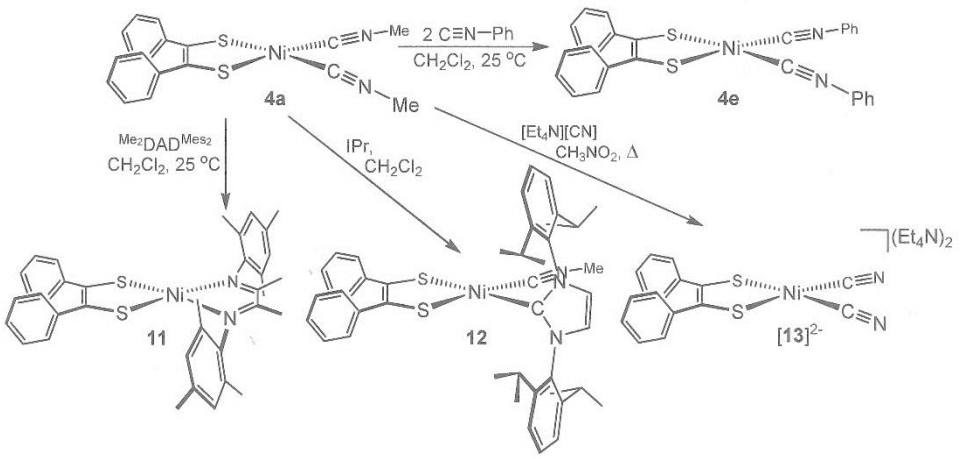

Scheme 4. Synthesis of monodithiolene compounds by substitution of MeNC from **4a**.

NO(*g*) or NH_3(*g*) to CH_2Cl_2 solutions of **1** leads to intractable brown solid, the result of ill-defined decomposition(s). Carbon monoxide, the quintessential π acid, notably fails to produce any reaction with **1** in chlorobenzene solutions heated to ~85 °C for 2 h. This observation indicates that the requisite ligand characteristic for dithiolene displacement is not π-acidity but rather σ basicity of the right degree. The absence of π-backbonding that is evident by the $\upsilon_{C\equiv N}$ values in **Table 3** for **4a-e**, **5a-e** and **6a-e** substantiates this notion. Both Me_4phen and $^{Me_2}DAD^{Mes_2}$ (**Scheme 2**) displace a dithiolene ligand from **1**, although the latter ligand forms only minor amounts of the dithiolene diimine complex in room temperature reactions. The modest amounts of **11** formed directly from **1** (~6%), compared to yields of ~70% for **10**, may arise from the ligand's preference for a *trans* disposition of the imine bonds about the diazadiene C−C single bond and consequently the existence of a barrier against the conformation that present both imine nitrogen atoms for chelation.[38]

The monodentate nature of the isonitrile ligands, the absence of metal-to-ligand π-backbonding in **4-6** evident by IR spectroscopy, and the relative volatility of MeN≡C collectively recommend **4a** for study as a synthon toward heteroleptic nickel dithiolene complexes that are not directly accessible from **1**, as shown in **Scheme 2**. The feasibility of MeN≡C substitution from **4a** is demonstrated by its facile and complete conversion to **4e** (**Scheme 4**). Compound **11** is formed from **4a** in yields of 67% under conditions that yielded only minor amounts from **1**. The identity of **11** was confirmed structurally by X-ray diffraction (**Figure 3**). Two eq of IPr (IPr = 1,3-bis(2,6-diisopropylphenyl)imidazol-2-ylidene) in reaction with **4a** produces mono-carbene, mono-isonitrile complex **12**, demonstrating an inability to accommodate two bulky carbene

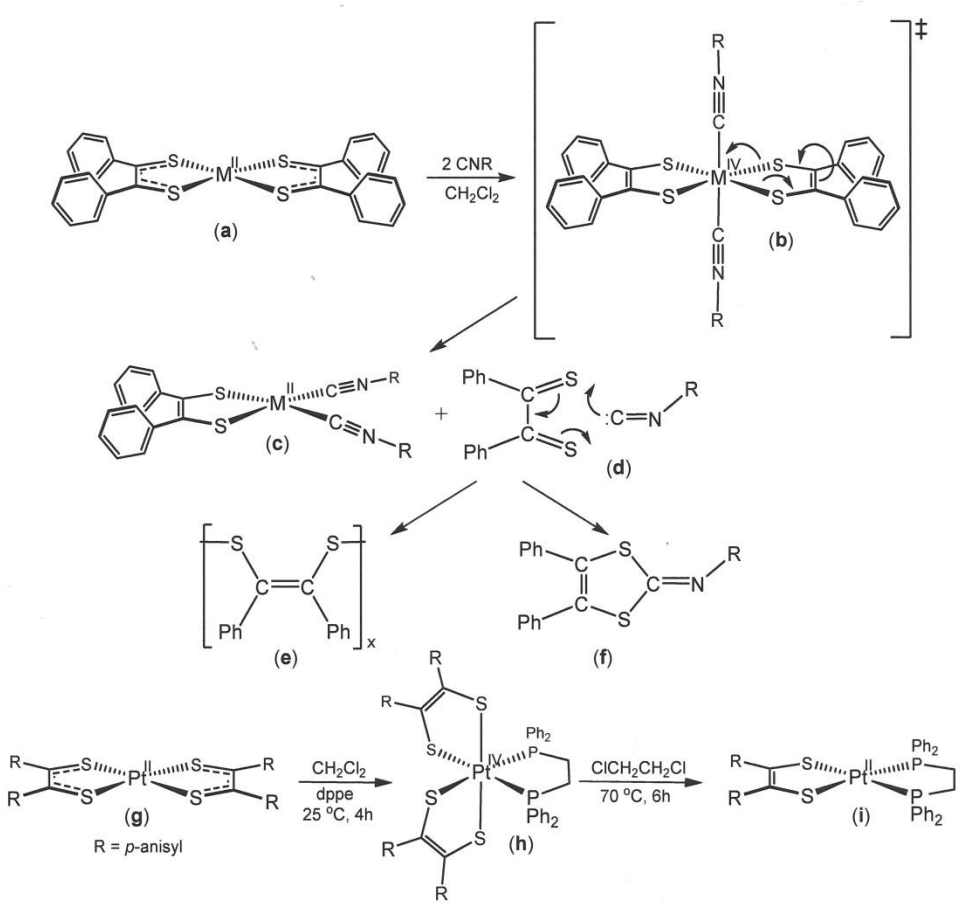

Scheme 5. Formation of dithiobenzil (**d**) as immediate, transient product of displacement by isonitrile and cycloaddition with excess isonitrile to form 4,5-diphenyl-1,3-dithiol-2-cyclohexylimine ((**f**), R = Cy). Displacement of dithiolene ligand by phosphine ((**g**) → (**i**)) is known to proceed via (**h**),[41] which suggests (**b**) as a plausible intermediate in the reaction of (**a**) with isonitriles.

ligands in a *cis* arrangement. The MeNC ligand in **12** is modestly bent away from the IPr ligand in response to its steric profile, which opens the C(15)−Ni(1)−C(42) angle to 94.4(2)° from a value of 89.91(5) in **4a**. The bis(cyanide) dianion [**13**]$^{2-}$ is accessible from **4a**, albeit via a modified preparation involving polar, non-coordinating CH_3NO_2 as solvent and the application of reduced pressure to remove displaced MeNC as a competing ligand. The structure of the [**13**]$^{2-}$ (**Figure 3** (**d**)) is square planar and highly similar to **4a** but with Ni–S and Ni–C bond lengths (**Table 2**) that are longer by ~0.015 Å. These increased bond distances likely arise from charge-repulsion effect from four anionic ligands in the coordination sphere. A related nickel compound in which the dithiolene chelate is incorporated to a tetrathiafulvalene system was prepared from

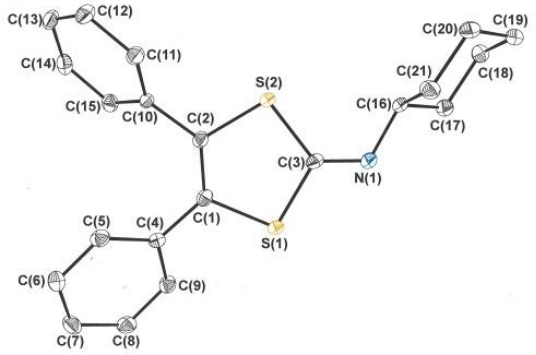

Figure 4. Thermal ellipsoid plot (50%) of 4,5-diphenyl-1,3-dithiol-2-cyclohexylimine. Hydrogen atoms are omitted for clarity.

$[Ni(CN)_4]^{2-}$ and the *in situ* generated ene-1,2-dithiolate and appears to be the only other Group 10 complex of the type.[39,40]

On the basis of abundant structural and spectroscopic data, the dithiolene ligands in **1** are unequivocally radical monoanions ((**b**), **Scheme 1**), while the ligand remaining in $[Ni(S_2C_2Ph_2)L_2]$ following substitution by L is an unambiguous ene-1,2-dithiolate dianion ((**a**), **Scheme 1**). Considerations of electron balance support formulating the departing dithiolene ligands as a fully oxidized α-dithione (**Scheme 5**, (**d**)), a form of the ligand whose inherent reactivity likely leads to rapid oligomerization ((**e**), **Scheme 5**). Reasoning that use of excess C≡N−R ligand under dilute conditions should promote its interception of the liberated dithione, the reaction of **1** with 4 eq of C≡N−Cy at micromolar concentration was indeed found to lead to modest, isolable quantities of 4,5-diphenyl-1,3-dithia-2-cyclohexylimine, which was identified structurally (**Figure 4**). Since the cycloaddition reaction illustrated in **Scheme 5** (**d**) is the obvious mechanism by which this heterocycle would form, its isolation is strongly, if not definitively, indicative of the formation of dithiobenzil.

In his early exploratory studies, Schrauzer did not consider the fate of the dithiolene ligand displaced from **1** by PR_3. In view of the evidence reported here for the fully oxidized state of the departing dithiolene ligand, it appears appropriate to classify the ligand-substitution reactions of **Scheme 2** as, fundamentally, net ligand redox disproportionation reactions. Substitution of dithiolene ligand from $[Pt(S_2C_2R_2)_2]$ (R = Me, *p*-anisyl) has been shown to proceed via association of phosphine to form six-coordinate bis(dithiolene) bis(phosphine) complexes that are isolable (**Scheme 5**, (**h**)).[41] This associative step is an atypical oxidative addition because two

$$3[Ni(S_2C_2(CF_3)_2]^0 + 6MeCN \longrightarrow 2[Ni(S_2C_2(CF_3)_2]^{1-} + [Ni(MeCN)_6]^{2+} + "(CF_3)_2C_2S_2" \quad \textbf{Eq 4}$$

$$[M(S\text{-}S)_2]^z + 2L \longrightarrow [L_2M(S\text{-}S)] + (S\text{-}S) \quad \textbf{Eq 5}$$

electrons move from the divalent metal ion to the dithiolene ligands, thereby forming ene-dithiolates from radical monoanions, rather than to the ligands that have been added. Reductive elimination leaves a square planar M(II) ion with a fully reduced ene-dithiolate (**Scheme 5**, (**i**)) and implicitly expels the second dithiolene ligand in a two-electron oxidized form. Although none has been observed, it is probable that the reactions of **1**-**3** with isonitriles and dithiooxamides similarly proceed through six-coordinate intermediates (**Scheme 5**, (**b**)). It is also likely that irreversible oligomerization of the extruded α-dithione provides the thermodynamic impetus for dithiolene ligand substitution in these reactions.

Related Group 10 bis(dithiolene) complexes with electron-deficient substituents such as -CF_3 and -CN have been observed by Dance and Miller to undergo, in the presence of halide anions, amines, and moderate donor solvents, dithiolene displacement reactions mediated by apparent dithiolene-ligand redox disproportionation.[42] Although none of the putative intermediates was observed, a multi-step mechanism was formulated involving first the substitution of dithiolene ligand and then a set of rapid electron-transfer reactions. Characterization of the process as net ligand redox disproportionation arose from the occurrence of both reduced bis(dithiolene) complex and oxidized free dithiolene ligand (detected spectroscopically) in the overall reaction, typified by **Eq 4**. Dance and Miller noted the similarity of **Eq 5**, their proposed first step, to the type of dithiolene ligand substitution reactions shown in **Scheme 2** but conceded that "the distribution of charge between the intermediate mixed ligand complex and the displaced dithiolene ligand is uncertain."[42] An absence of the insights that are now offered by modern physical methods and DFT computations prevented Dance and Miller from recognizing **Eq 5** and reactions of the type in **Scheme 2** as ligand redox disproportionation reactions themselves.

In summary, this report maps out more fully the landscape of possible dithiolene ligand substitution reactions from $[M(S_2C_2R_2)_2]$ (M = Ni^{2+}, Pd^{2+}, Pt^{2+}), which until now has been limited only to substitution by phosphines and diimines. Isonitrile ligands of all types effectively displace one of two dithiolene ligands to afford a new group of organometallic dithiolene complexes. Similarly, dithiooxamides such as $^{i}Pr_2$pipdt yield dithiolate-dithione "push-pull" complexes in a direct and efficient manner. The feasibility of these reactions likely arises from

the dithiolene ligand's capacity to exert its redox non-innocence in supporting formation of the transient intermediates $[M^{IV}(^{-2}S_2C_2Ph_2)_2(C{\equiv}NR)_2]$ and $[M^{IV}(^{-2}S_2C_2Ph_2)_2(^{i}Pr_2pipdt)]$ from $[M^{II}(^{\bullet}S,^{-}SC_2Ph_2)]$. Because these putative intermediates entail two-electron redox chemistry *between dithiolene ligand and metal* in a net non-redox step, the system adheres to the notion that redox non-innocence be a behavior or property involving a combination of both metal and ligand.[43] Ultimately, reductive elimination of α-dithione from $[M^{IV}(^{-2}S_2C_2Ph_2)(C{\equiv}NR)_2]$ occurs in what amounts to a net dithiolene redox disproportionation. Although proposed decades earlier by Dance to account for the decomposition of electron-deficient bis(dithiolene) complexes in the presence of weak nucleophiles such as nitriles, amines, and halide anions, such redox disproportionation appears not to have been recognized as being pertinent to the dithiolene displacement reactions that yield isolable heteroleptic dithiolene complexes. Importantly, in instances where **1** is not amenable to direct dithiolene substitution, methylisonitrile complex **4a** promises to be useful as an entry point to new heteroleptic dithiolene compounds, such as the mono-carbene compound **12** and dicyanide anion $[\mathbf{13}]^{2-}$. Following reports will elaborate upon the syntheses, structures, properties and applications of these new sets of compounds.

Supporting Information

The Supporting Information is available free of charge on the ACS Publications website at DOI. X-ray data collection procedures, figures of crystallographically characterized compounds with full atom labeling, complete crystal data (CIF). CCDC deposition codes: $[Et_4N][\mathbf{1}]$, 1553819; **4a** 1547459; **5b**, 1547460; **6e**, 1547461; **7**, 1547462; **11**, 1547463; **12**·$ClCH_2CH_2Cl$, 1547464; $[Et_4N]_2[\mathbf{13}]$, 1553820; 4,5-diphenyl-1,3-dithiol-2-cyclohexylimine, 1547465.

Acknowledgments‡

The Louisiana Board of Regents (grant LEQSF-(2002-03)-ENH-TR-67) and NSF (MRI: 1228232; MRI: 0619770) are thanked for instrumentation support. Tulane University is acknowledged for its support of the X-ray diffraction facility.

References

(**1**) Sproules, S. Tris(dithiolene) Chemistry: A Golden Jubilee. *Prog. Inorg. Chem.* **2014**, *58*, 1-144.

(**2**) Eisenberg, R.; Gray, H. B. Noninnocence in Metal Complexes: A Dithiolene Dawn. *Inorg. Chem.* **2011**, *50*, 9741-9751.

(**3**) Lim, B. S.; Fomitchev, D. V.; Holm, R. H. Nickel Dithiolenes Revisited: Structures and Electronic Distribution from Density Functional Theory for the Three-Member ElectronTransfer Series $[Ni(S_2C_2Me_2)_2]^{0,1-,2-}$. *Inorg. Chem.* **2001**, *40*, 4257-4262.

(**4**) Bigoli, F.; Chen, C.-T.; Wu, W.-C.; Deplano, P.; Mercuri, M. L.; Pellinghelli, M. A.; Pilia, L.; Pintus, G.; Serpe, A.; Trogu, E. F. $[Ni(R_2pipdt)_2](BF_4)_2$ (R_2pipdt = 1,4-Disubstituted-piperazine-3,2-dithione) as Useful Precursors of Mixed-Ligand Dithiolenes of Interest for Non-Linear Optics. *Chem. Commun.* **2001**, 2246-2247.

(**5**) Davison, A.; Edelstein, N.; Holm, R. H.; Maki, A. H. Further Examples of Complexes Related by Electron-Transfer Reactions: Complexes Derived from Bis(trifluoromethyl)-1,2-Dithietene. *Inorg. Chem.* **1964**, *3*, 814-823.

(**6**) Schrauzer, G. N.; Mayveg, V. P. Preparation, Reactions, and Structure of Bisdithio-α-diketone Complexes of Nickel, Palladium, and Platinum. *J. Am. Chem. Soc.* **1965**, *83*, 1483-1489.

(**7**) Miller, T. R.; Dance, I. G. Reactions of Dithiolene Complexes with Amines. II. The Formation and Properties of Mixed-Ligand Dithiolene α-Diimine Complexes of Nickel. *J. Am. Chem. Soc.***1973**, *95*, 6970-6979.

(**8**) Chen, C.-T.; Liao, S.Y.; Lin, K.-J.; Chen, C. H.; Lin, T.-Y. J. Structural Effects on Molecular Dipoles and Solvatochromism of Nickel(diimine)(dithiolate) Complexes. *Inorg. Chem.* **1999**, *38*, 2734-2741.

(**9**) Kumar, A.; Auvinem, S.; Trivendi, M.; Chauhan, R.; Alatalo, M. Synthesis, Characterization and Light Harvesting Properties of Nickel(II) Diimine Dithiolate Complexes. *Spectrochim Acta, Part A* **2013**, *115*, 106-110.

(**10**) Pollock, C. J.; Tan, L. L.; Zhang, W.; Lancaster, K. M.; Lee, S. C.; DeBeer, S. Light Atom Influences on the Electronic Structures of Iron-Sulfur Clusters. *Inorg. Chem.* **2014**, *53*, 2591-2597.

(**11**) George, G. N. *EXAFSPAK*; Stanford Synchrotron Radiation Laboratory, Stanford Linear Accelerator Center, Stanford University: Stanford, CA, 2001.

(**12**) Schuster, R. E.; Scott, J. E.; Casanova, Jr., J. Methyl Isocyanide. *Org. Syn.* **1966**, *46*, 75-77.

(**13**) Gokel, G. W.; Widera, R. P.; Weber, W. P. Phase-Transfer Hofmann Carbylamine Reaction: *tert*-Butyl Isocyanide. *Org. Syn.* **1976**, *55*, 96-99.

(**14**) Isaksson, R.; Liljefors, T.; Sandström, J. Synthesis of Some Five-, Six- and Seven-Membered Cyclic Oxamides and Their Mono- and Di-thio Analogues. *J. Chem. Research (S).* **1981**, 43.

(**15**) Bantreil, X.; Nolan, S. P. Synthesis of *N*-Heterocyclic Carbene Ligands and Derived Ruthenium Olefin Metathesis Catalysts. *Nat. Protoc.* **2011**, *6*, 69-77.

(**16**) Connelly, N. G.; Crossley, J. G.; Orpen, A. G. Linear Chain Metal Compounds: $[M(mnt)(CNMe)_2]$[M = Ni, Pd, Pt; mnt = $1,2\text{-}S_2C_2(CN)_2$]. *J. Chem. Soc., Chem. Commun.* **1992**, 1568-1571.

(**17**) Miller, J. S.; Balch, A. L. Preparation and Reactions of Tetrakis(methyl isocyanide) Complexes of Divalent Nickel, Palladium, and Platinum. *Inorg. Chem.* **1972**, *11*, 2069-2074.

(**18**) Connelly, N. G.; Crossley, J. G.; Orpen, A, G.; Salter, H. The Co-stacking of a Planar Metal Complex and a Novel 1,3-Dithiole: The Synthesis and Crystal Structure of $[Pt(mnt)(CNMe)_2]\cdot(NC)_2C_2S_2CNMe$. *J. Organomet. Chem.* **1994**, *480*, C12-C13.

(**19**) Donahue, J. P.; Goldsmith, C. R.; Nadiminti, U.; Holm, R. H. Synthesis, Structures, and Reactivity of Bis(dithiolene)molybdenum(IV,VI) Complexes Related to the Active Sites of Molybdoenzymes. *J. Am. Chem. Soc.* **1998**, *120*, 12869-12881.

(**20**) Yan, Y.; Keating, C.; Chandrasekaran, P.; Jayarathne, U.; Mague, J. T.; DeBeer, S.; Lancaster, K. M.; Sproules, S.; Rubtsov, I. V.; Donahue, J. P. Ancillary Ligand Effects upon Dithiolene Redox Noninnocence in Tungsten Bis(dithiolene) Complexes. *Inorg. Chem.* **2013**, *52*, 6743-6751.

(**21**) Eckenhoff, W. T.; Brennessel, W. W.; Eisenberg, R. Light-Driven Hydrogen Production from Aqueous Protons using Molybdenum Catalysts. *Inorg. Chem.* **2014**, 53, 9860-9869.

(**22**) Lorber, C.; Donahue, J. P.; Goddard, C. A.; Nordlander, E.; Holm, R. H. Synthesis, Structures, and oxo Transfer Reactivity of Bis(dithiolene)tungsten(IV,VI) Complexes Related to the Active Stites of Tungstoenzymes. *J. Am. Chem. Soc.* **1998**, *120*, 8102-8112.

(**23**) Mashima, K.; Kaneyoshi, H.; Kaneko, S.; Mikami, A.; Tani, K.; Nakamura, A. Chemistry of Coordinatively Unsaturated Bis(thiolato)ruthenium(II) Complexes (η^6-arene)$Ru(SAr)_2$ [SAr = 2,6-Dimethylbenzenethiolate, 2,4,6-Triisopropylbenzenethiolate; $(SAr)_2$ = 1,2-Benzenedithiolate; Arene = Benzene, *p*-Cymene, Hexamethylbenzene]. *Organometallics* **1997**, *16*, 1016-1025.

(**24**) Cotton, F. A.; Zingales, F. The Donor-Acceptor Properties of Isonitriles as Estimated by Infrared Study. *J. Am. Chem. Soc.* **1961**, *83*, 351-355.

(**25**) Ray, K.; DeBeer George, S.; Solomon, E. I.; Wieghardt, K.; Neese, F. Description of the Ground State Covalencies of the Bis(dithiolato) Transition-Metal Complexes from X-Ray Absorption Spectroscopy and Time-Dependent Density-Functional Calculations. *Chem. Eur. J.* **2013**, *13*, 2783-2797.

(**26**) Cummings, S. D.; Eisenberg, R. Luminescence and Photochemistry of Metal Dithiolene Complexes. *Prog. Inorg. Chem.* **2004**, *52*, 315-367.

(**27**) Islam, A.; Sugihara, H.; Hara, K.; Singh, L. P.; Katoh, R.; Yanagida, M.; Takahashi, Y.; Murata, S.; Arakawa, H. Dye Sensitization of Nanocrystalline Titanium Dioxide with Square Planar Platinum(II) Diimine Dithiolate Complexes. *Inorg. Chem.* **2001**, *40*, 5371-5370.

(**28**) Geary, E. A. M.; Hirata, N.; Clifford, J.; Durrant, J. R.; Parsons, S.; Dawson, A.; Yellowlees, L. J.; Robertson, N. Synthesis, Structures and Properties of [Pt(2,2´-bipyridyl-5,5´-dicarboxylic acid)(3,4-toluenedithiolate)]: Tuning Molecular Properties for Application in Dye-Sensitized Solar Cells. *Dalton Trans.* **2003**, 3757-3762.

(**29**) Geary, E. A. M.; Yellowlees, L. J.; Jack, L. A.; Oswald, I. D. H.; Parsons, S.; Hirata, N.; Durrant, J. R.; Robertson, N. Synthesis, Structure, and Properties of [Pt(II)(diimine)(dithiolate)] Dyes with 3,3´-, 4,4´-, 5,5´-Disubstituted Bipyridyl: Applications in Dye-Sensitized Solar Cells. *Inorg. Chem.* **2005**, *44*, 242-250.

(**30**) Hissler, M.; McGarrah, J. E.; Connick, W. B.; Geiger, D. K.; Cummings, D. K.; Cummings, S. D.; Eisenberg, R. Platinum Diimine Complexes: Towards a Molecular Photochemical Device. *Coord. Chem. Rev.* **2000**, *20*8, 115-137.

(**31**) Zhang, J.; Du, P.; Schneider, J.; Jarosz, P.; Eisenberg, R. Photogeneration of Hydrogen from Water Using an Integrated System Based on TiO_2 and Platinum(II) Diimine Dithiolate Sensitizers. *J. Am. Chem. Soc.* **2007**, *129*, 7726-7727.

(**32**) Zheng, B.; Sabatini, R. P.; Fu, W.-F.; Brennessel, W. W.; Wang, L.; mcCamant, D. W.; Eisenberg, R. Light-Driven Generation of Hydrogen: New Chromophore Dyads for Increased Activity Based on Bodipy Dye and Pt(diimine)(dithiolate) Complexes. *Proc. Natl Acad. Sci. U. S. A.* **2015**, *12*, E3987-E3996.

(**33**) Pilato, R. S.; van Houten, K. A. Metal Dithiolene Complexes in Detection: Past, Present, and Future. *Prog. Inorg. Chem.* **2004**, *52*, 369-397.

(**34**) Espa, D.; Pilia, L.; Marchiò, L.; Mercuri, M. L.; Serpe, A.; Barsella, A.; Fort, A.; Dalgleish, S. J.; Robertson, N.; Deplano, P. Redox-Switchable Chromophores Based on Metal (Ni, Pd, Pt) Mixed-Ligand Dithiolene Complexes Showing Molecular Second-Order Nonlinear-Optical Activity. *Inorg. Chem.* **2011**, *50*, 2058-2060.

(**35**) Pilia, L.; Espa, D.; Barsella, A.; Fort, A.; Makedonas, C.; Marchiò, L.; Mercuri, M. L.; Serpe, A.; Mitsopoulou, C. A.; Deplano, P. Combined Experimental and Theoretical Study on Redox-Active d^8 Metal Dithione-Dithiolato Complexes Showing Molecular Second-Order Nonlinear Optical Activity. *Inorg. Chem.* **2011**, *50*, 10015-10027.

(**36**) Espa, D.; Pilia, L.; Makedonas, C.; Marchiò, L.; Mercuri, M. L.; Serpe, A.; Barsella, A.; Fort, A.; Mitsopoulou, C. A.; Deplano, P. Role of the Acceptor in Tuning the Properties of Metal [M(II) = Ni, Pd, Pt] Dithiolato/Dithione (Donor/Acceptor) Second-Order Nonlinear Chromophores: Combined Experimental and Theoretical Studies. *Inorg. Chem.* **2014**, *53*, 1170-1183.

(**37**) Rajalakshmi, A.; Radha, A.; Seshasayee, M.; Kuppuswamy, P.; Manoharan, P. T. Crystal and Molecular Structure of Tetraethylammonium Bis(stilbene-1,2-dithiolato) Nickelate(III). *Z. Kristallogr.* **1989**, *187*, 159-164.

(**38**) Schaub, T.; Radius, U. A Diazabutadiene Stabilized Nickel(0) Cyclooctadiene Complex: Synthesis, Characterization and the Reaction with Diphenylacetylene. *Z. Anorg. Allg. Chem.* **2006**, *632*, 807-813.

(**39**) Naito, T.; Kobayashi, N.; Inabe, T. Synthesis of New Ni-Complexes with a Chalcogen Donor Ligand and Cyano Groups. *Chem. Lett.* **1998**, *27*, 723-724.

(**40**) Naito, T.; Kobayashi, N.; Inabe, T. Preparation of a New Conducting and Magnetic Material Based on Coordination Compounds. *Synth. Met.* **1999**, *102*, 1687-1688.

(**41**) Chandrasekaran, P.; Greene, A. F.; Lillich, K.; Capone, S.; Mague, J. T.; DeBeer, S.; Donahue, J. P. A Structural and Spectroscopic Investigation of Octahedral Platinum Bis(dithiolene) Phosphine Complexes: Phosphine Association Enabled by Platinum-Dithiolene Internal Redox Chemistry. *Inorg. Chem.* **2014**, *53*, 9192-9205.

(**42**) Dance, I. G.; Miller, T. R. Ready Displacement of Dithiolene Ligands from Electron-poor Dithiolene Complexes by Weak Nucleophiles. *J. Chem. Soc., Chem. Commun.* **1976**, 112-113.

(**43**) Ward, M. D.; McCleverty, J. A. Non-innocent Behaviour in Mononuclear and Polynuclear Complexes: Consequences for Redox and Electronic Spectroscopic Properties. *Dalton Trans.* **2002**, 275-288.

For Table of Contents Only

Expanding the Scope of Ligand Substitution from $[M(S_2C_2Ph_2]$ (M = Ni^{2+}, Pd^{2+}, Pt^{2+}) to Afford New Classes of Heteroleptic Dithiolene Complexes

Antony Obanda, Kristina Martinez, Russell H. Schmehl, Joel T. Mague, Igor V. Rubtsov, Samantha N. MacMillan, Kyle M. Lancaster, Stephen Sproules and James P. Donahue*

The scope of dithiolene substitution from $[M(S_2C_2Ph_2)_2]$ (M = Ni^{2+}, Pd^{2+}, Pt^{2+}) to produce $[M(S_2C_2Ph_2)L_n]$ (*n* = 1, 2) has been broadened to include isonitriles and dithiooxamides in addition to phosphines and dimines, all of them relatively soft σ donors. Substitution of dithiolene is enabled by redox disproportionation of the dithiolene ligands from radical monoanions to ene-dithiolate and dithione, the latter of which is an enhanced leaving group that is subject to further irreversible reactions.

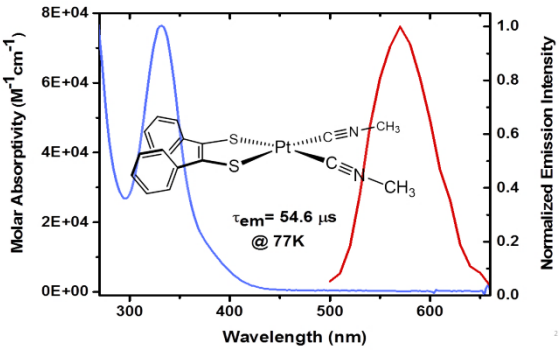

Supporting Information

for

Expanding the Scope of Ligand Substitution from $[M(S_2C_2Ph_2)_2]$ ($M = Ni^{2+}$, Pd^{2+}, Pt^{2+}) to Afford New Heteroleptic Dithiolene Complexes

Antony Obanda[†] Kristina Martinez,[†] Russell H. Schmehl,[†] Joel T. Mague,[†] Igor V. Rubtsov,[†] Samantha N. MacMillan,[£] Kyle M. Lancaster,[£] Stephen Sproules[§] and James P. Donahue*[,†]

Table of Contents

[†]Dept. of Chemistry, Tulane University, 6400 Freret Street, New Orleans, LA 70118-5698, U.S.A.
[£]Dept. of Chemistry and Chemical Biology, Cornell University, 162 Science Dr., Ithaca, New York 14853, U.S.A.
[§]School of Chemistry, University of Glasgow, University Avenue, Glasgow, Lanarkshire, G12 8QQ, U.K.

Procedures for Crystal Growth, Collection and Processing of Diffraction Data, and Solving and Refining of Structures.

Diffraction-quality crystals of most of the compounds identified by X-ray diffraction were obtained by vapor diffusion techniques. The following solvent pairs provide specific combinations successfully implemented as solvent/diffusing vapor for crystal growth: **4a** (CH_2Cl_2/Et_2O), **5c** (CH_2Cl_2/Et_2O), **6e** (CH_2Cl_2/*n*-pentane), **7** (CH_2Cl_2/Et_2O), **11** (CH_2Cl_2/Et_2O), **12**·($ClCH_2CH_2Cl$) ($ClCH_2CH_2Cl$/hexanes), 4,5-diphenyl-1,3-dithiol-2-cyclohexylimine (CH_2Cl_2/hexanes). A layered diffusion of Et_2O onto a MeCN solution was employed for the crystallization of $[Et_4N]_2[Ni(S_2C_2Ph_2)(CN)_2]$, while slow evaporation of a CH_2Cl_2 solution of $[Et_4N][Ni(S_2C_2Ph_2)_2]$ afforded a crystalline sample suitable for diffraction. The color and morphology of each crystal are presented in **Table 1** of the manuscript.

All crystals were coated with paratone oil and mounted on the end of a nylon loop attached to the end of the goniometer. Except for **7**, for which data were obtained at 100 K with a Bruker D8 Venture Photon 100 instrument, data were collected with a Bruker Smart APEX CCD diffractometer equipped with a Kryoflex attachment supplying a nitrogen stream at 100 K or 150 K. The radiation source employed by the D8 Venture was a Cu Incoatec I microfocus source generating X-rays with λ = 1.54178 nm, while the Smart APEX operated with a Mo fine-focus sealed tube providing radiation at λ = 0.71073 nm. An assemblage of six sets of ω-scan frames comprising a hemisphere of data were collected for **7** using 10 second frame times. All data sets gathered using the Smart APEX CCD instrument employed a collection routine comprised of three sets of 400 frames in ω (0.5º/scan), collected at φ = 0.00, 90.00 and 180.00° and two sets of 800 frames in φ (0.45°/scan) collected with ω constant at -30.00 and 210.00°. The frame time used for these data sets were as follows: $[Et_4N]$[**1**] (20 sec), **4a** (10 sec), **5c** (30 sec), **6e** (15 sec), **7** (15 sec), **11** (30 sec), **12**·(25 sec), $[Et_4N]_2$[**13**] (20 sec), 4,5-diphenyl-1,3-dithiol-2-cyclohexylimine (30 sec).

All data were collected under control of either the *APEX2*[1] or *APEX3*[2] software package. Raw data were reduced to F^2 values using *SAINT*[3], and a global refinement of unit cell parameters was performed using ~8000–10,000 selected reflections from the full data set. In the case of **7**, a somewhat smaller set of 6802 reflections was used for the unit cell refinement. Data were corrected for absorption on the basis of multiple measurements of symmetry equivalent reflections with the use of *SADABS*,[4] All structure solutions were obtained by direct methods

using *SHELXT*,[5] while refinements were accomplished by full-matrix least-squares procedures using *SHELXL*.[6] Both the *SHELXS* and *SHELXL* programs are incorporated into the *SHELXTL*[7] and *APEX2*[1], *APEX3*[2] software suites.

All structure refinements were routine and required no special treatment. Hydrogen atoms were added in calculated positions and included as riding contributions with isotropic displacement parameters tied to those of the carbon atoms to which they were attached. Thermal ellipsoid images have been created with the use of *XP*, which also is part of the *SHELXTL* package. All structures were checked for overlooked symmetry and other errors by the checkCIF service provided by the International Union of Crystallography.[8] Final unit cell data and refinement statistics are collected in **Table 1** of the manuscript.

References

(**1**) *APEX2*, Bruker-AXS, Inc., Madison, Wisconsin, USA, 2015.

(**2**) *APEX3*, Bruker-AXS, Inc., Madison, Wisconsin, USA, 2016.

(**3**) (a) *SAINT*, Bruker AXS, Inc., Madison, Wisconsin, 2015. (b) *SAINT*, Bruker AXS, Inc., Madison, Wisconsin, 2016.

(**4**) (a) Sheldrick, G. M. *SADABS*, Universität Göttingen, Göttingen, Germany, 2015. (b) Sheldrick, G. M. *SADABS*, Universität Göttingen, Göttingen, Germany, 2016.

(**5**) Sheldrick, G. M. *"SHELXT – Integrated Space-Group and Crystal-Structure Determination." Acta Crystallogr., Sect A* **2015**, *71*, 3-8.

(**6**) (**a**) Sheldrick, G. M. *SHELXL*, Acta *Crystallogr., Sect A* **2015**, *71*, 3-8. (**b**) Sheldrick, G. M. *SHELXL-2014/7*, Acta *Crystallogr., Sect A* **2015**, *71*, 3-8.

(**7**) (a) *SHELXTL*, Bruker-AXS, Madison, WI, 2015. (b) *SHELXTL*, Bruker-AXS, Madison, WI, 2016.

(**8**) See http://checkcif.iucr.org/

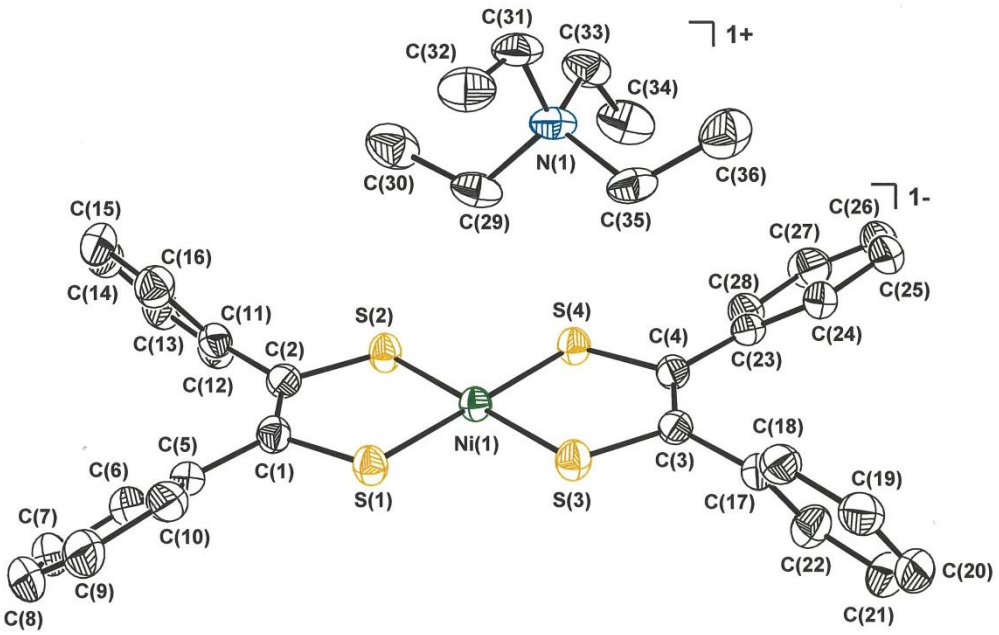

Figure S1. Full atom labeling for the $[Et_4N][Ni(S_2C_2Ph_2)_2]$, $[Et_4N][$**1**$]$. The thermal ellipsoid plot is drawn at the 50% level. Hydrogen atoms are omitted for clarity.

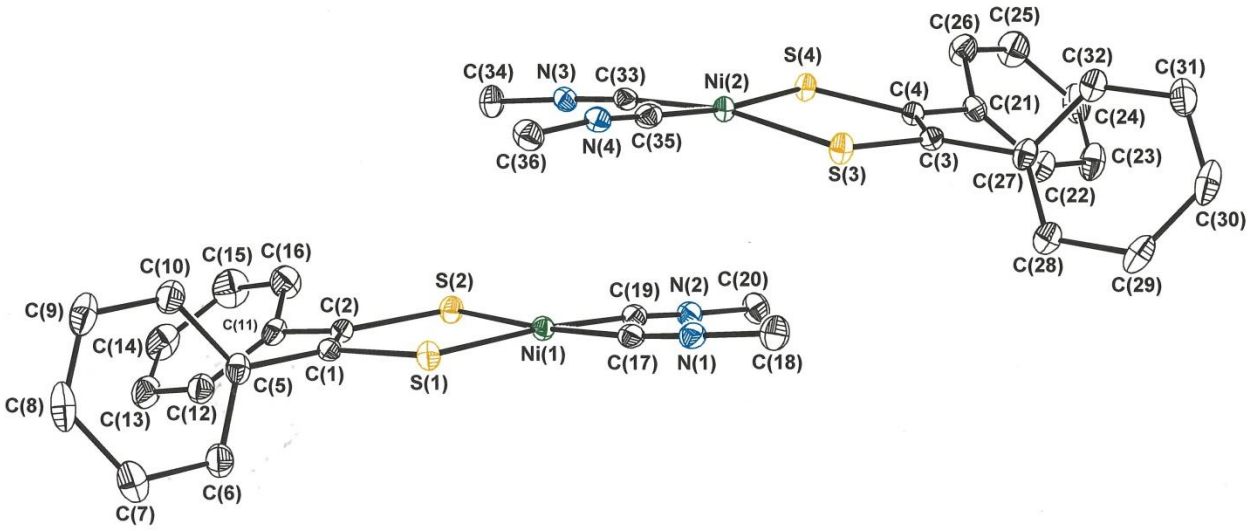

Figure S2. Full atom labeling for the two independent molecules of $[(Ph_2C_2S_2)Ni(C{\equiv}NMe)_2]$, **4a**. The thermal ellipsoid plot is drawn at the 50% level. Hydrogen atoms are omitted for clarity.

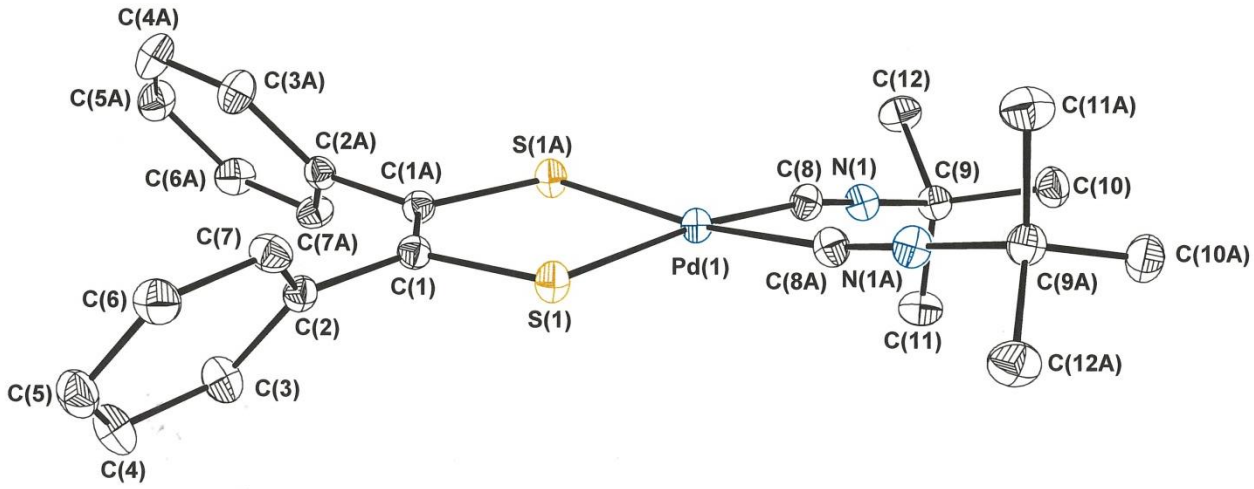

Figure S3. Atom labeling for [$(Ph_2C_2S_2)Pd(C{\equiv}N^tBu)_2$], **5c**. The thermal ellipsoid plot is shown at the 50% probability level, and all hydrogen atoms are omitted for clarity.

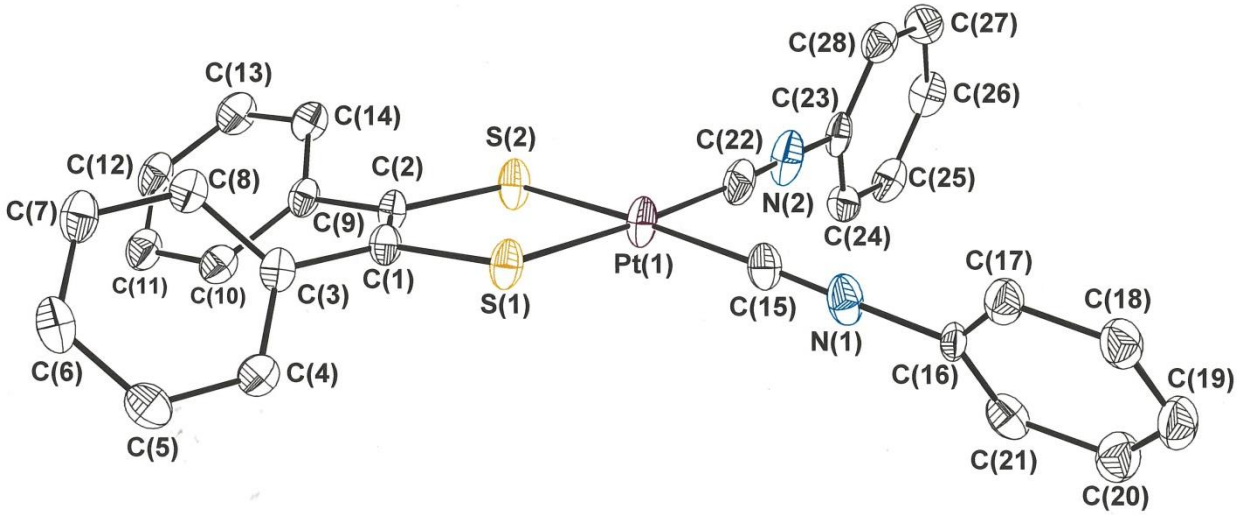

Figure S4. Atom labeling for [$(Ph_2C_2S_2)Pt(C{\equiv}NPh)_2$], **6e**. The thermal ellipsoid plot is shown at the 50% probability level, and all hydrogen atoms are omitted for clarity.

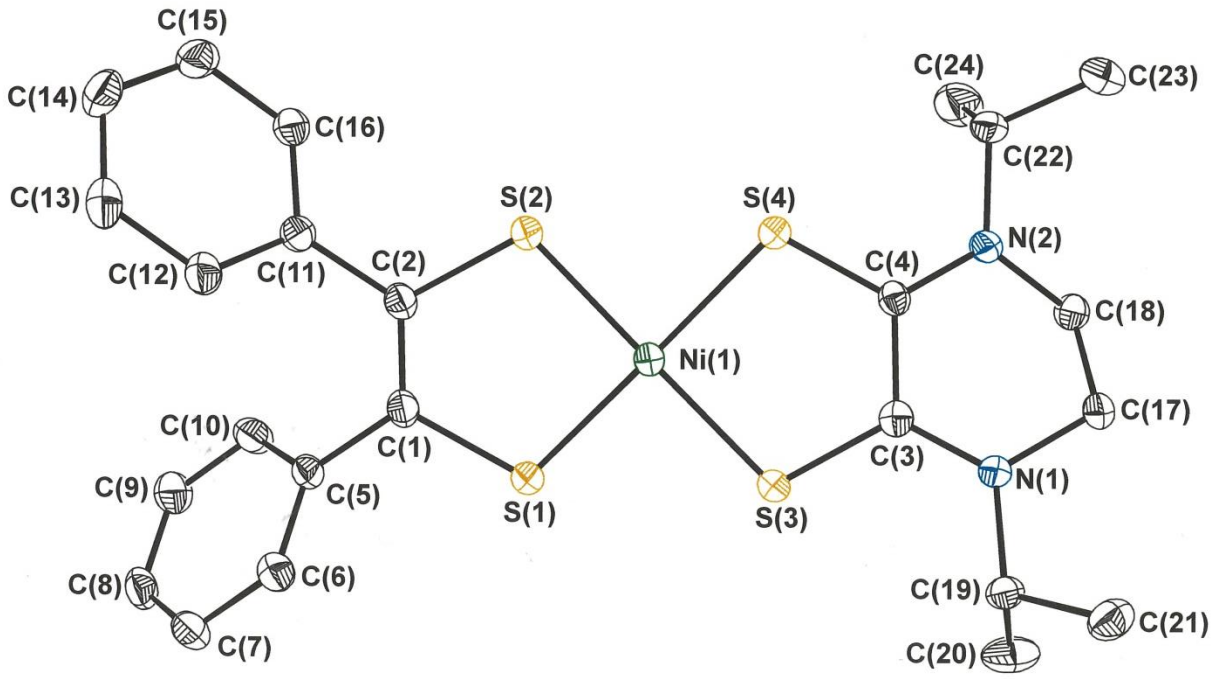

Figure S5. Complete atom labeling for [Ni($S_2C_2Ph_2$)($^{i}Pr_2$pipdt)], **7**. The thermal ellipsoid plot is drawn at the 50% level, and all hydrogen atoms are omitted for clarity.

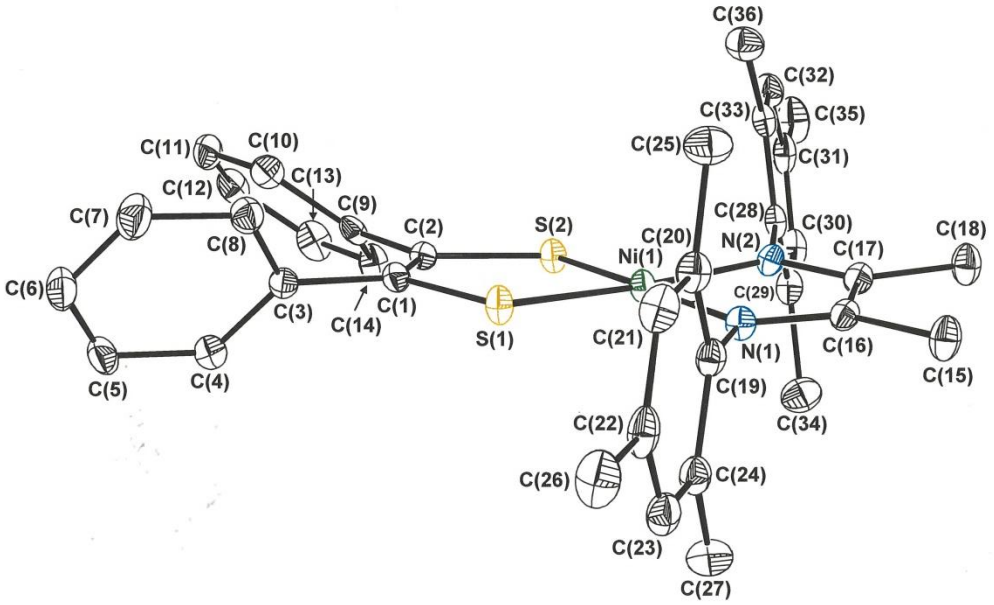

Figure S6. Complete atom labeling for [Ni($S_2C_2Ph_2$)(^{Me_2}DAD^{Mes_2})], **11** The thermal ellipsoid plot is presented at the 50% probability level, and all hydrogen atoms are omitted for clarity.

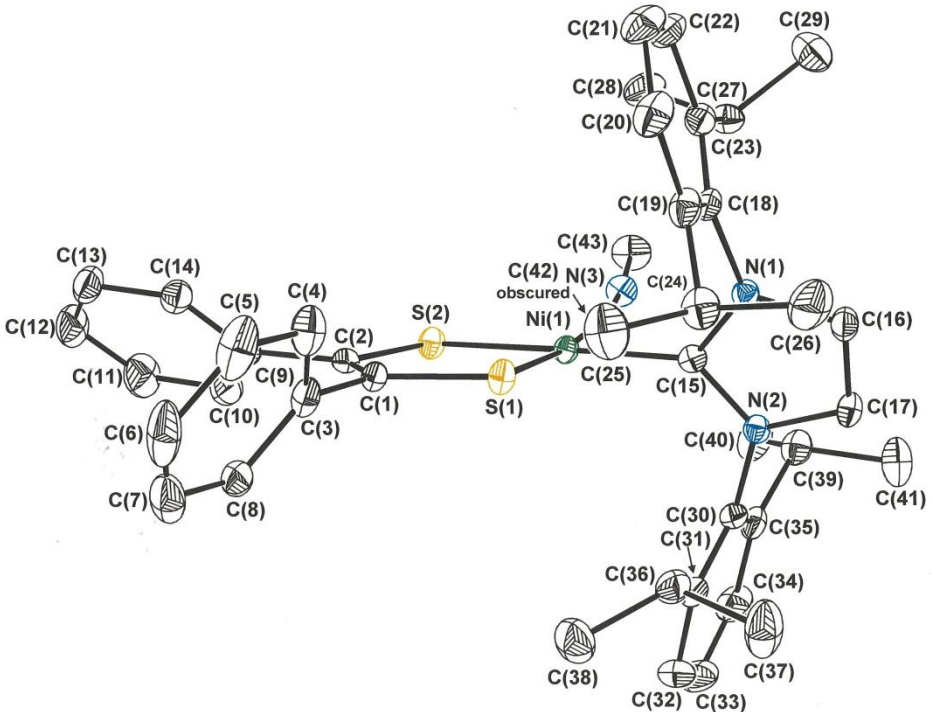

Figure S7. Complete atom labeling for [Ni($S_2C_2Ph_2$)(IPr)(C≡NMe)], **12**. The thermal ellipsoid plot is drawn at the 50% probability level, and all hydrogen atoms have been omitted for greater clarity.

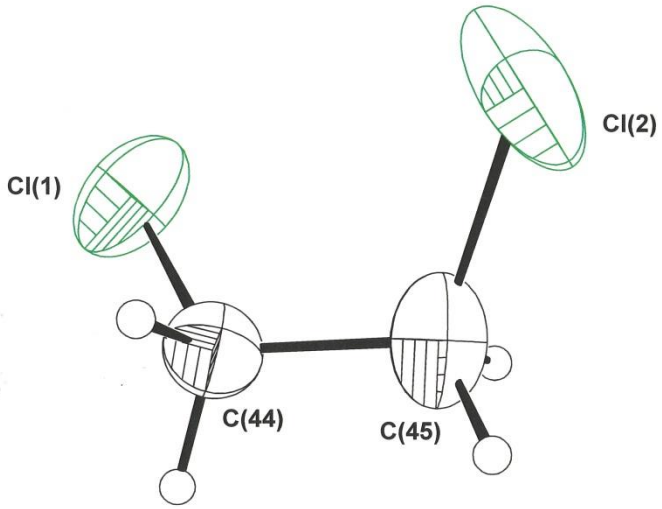

Figure S8. Complete atom labeling for the 1,2-dichloroethane interstitial solvent in [Ni($S_2C_2Ph_2$)(IPr)(C≡NMe)]·$ClCH_2CH_2Cl$. The thermal ellipsoid plot is drawn at the 50% probability level.

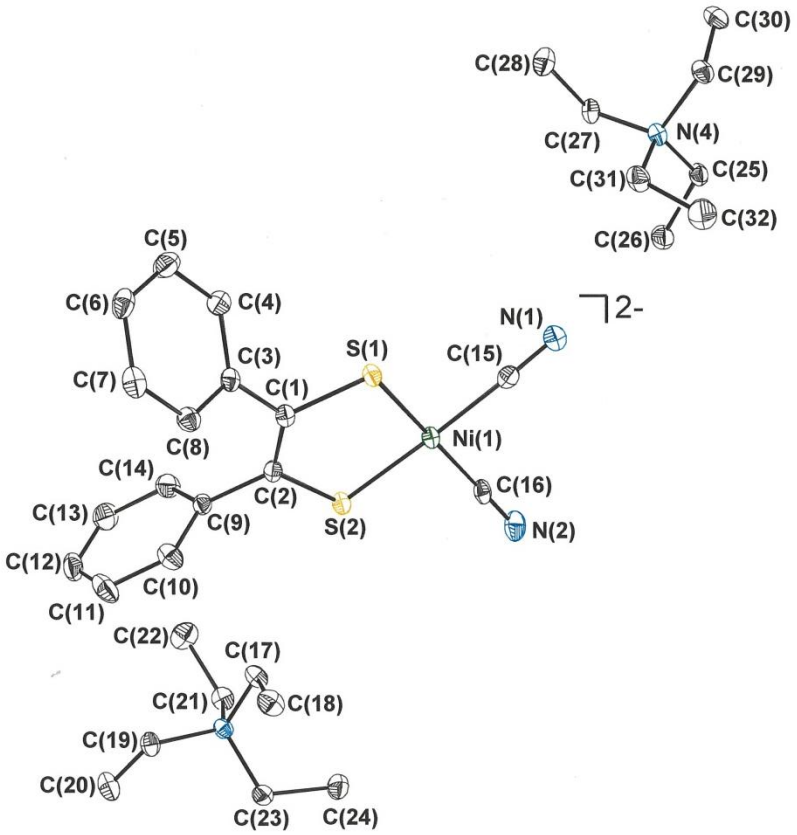

Figure S9. Complete atom labeling for $[Et_4N]_2[Ni(S_2C_2Ph_2)(CN)_2]$, $[Et_4N]_2$[**13**]. The thermal ellipsoid plot is drawn at the 50% probability level. All hydrogen atoms are omitted for clarity.

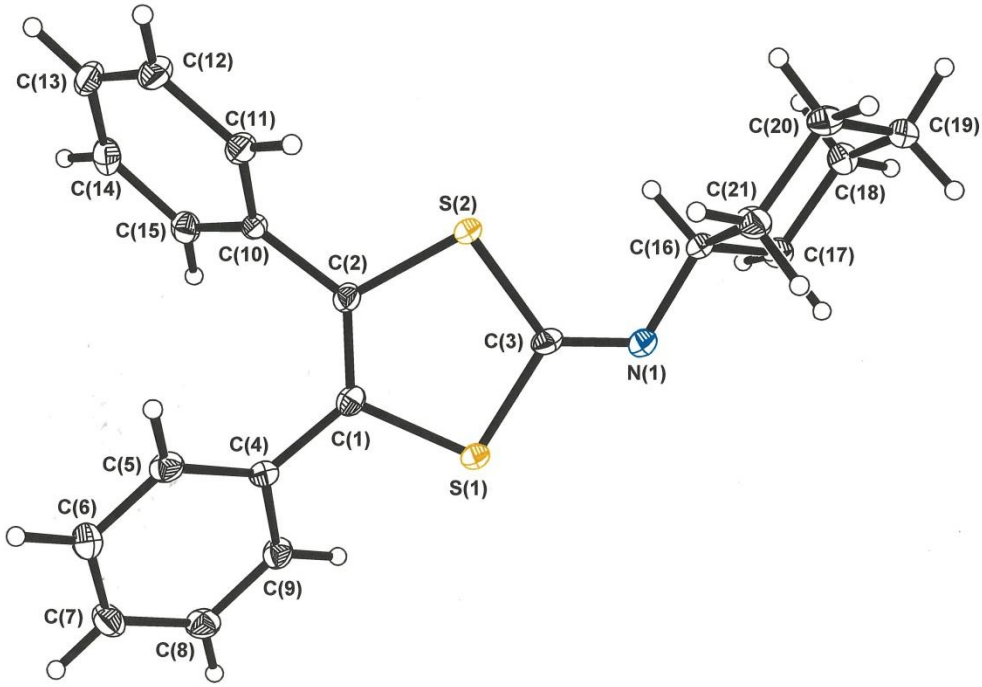

Figure S10. Complete atom labeling for 4.5-dimethyl-1,3-dithiol-2-cyclohexylimine. The thermal ellipsoid plot is drawn at the 50% level.